1977-03

An investigation of the recovery processes in 7075-T651 aluminum responsible for a stress decay during dynamic loading histories

Bentley, Richard Allen

Monterey, California. Naval Postgraduate School

NAVAL POSTGRADUATE SCHOOL
Monterey, California

THESIS

An Investigation of the Recovery Processes in 7075-T651 Aluminum Responsible for a Stress Decay During Dynamic Loading Histories

by

Richard Allen Bentley

March 1977

Thesis Advisor: G. H. Lindsey

REPORT DOCUMENTATION PAGE

READ INSTRUCTIONS BEFORE COMPLETING FORM

1. REPORT NUMBER	2. GOVT ACCESSION NO. / 3. RECIPIENT'S CATALOG NUMBER
4. TITLE (and Subtitle): An Investigation of the Recovery Processes in 7075-T651 Aluminum Responsible for a Stress Decay During Dynamic Loading Histories	5. TYPE OF REPORT & PERIOD COVERED: Master's Thesis; March 1977 / 6. PERFORMING ORG. REPORT NUMBER
7. AUTHOR(s): Richard Allen Bentley	8. CONTRACT OR GRANT NUMBER(s)
9. PERFORMING ORGANIZATION NAME AND ADDRESS: Naval Postgraduate School, Monterey, California 93940	10. PROGRAM ELEMENT, PROJECT, TASK AREA & WORK UNIT NUMBERS
11. CONTROLLING OFFICE NAME AND ADDRESS: Naval Postgraduate School, Monterey, California 93940	12. REPORT DATE: March 1977 / 13. NUMBER OF PAGES: 101
14. MONITORING AGENCY NAME & ADDRESS (if different from Controlling Office): Naval Postgraduate School, Monterey, California 93940	15. SECURITY CLASS. (of this report): UNCLASSIFIED / 15a. DECLASSIFICATION/DOWNGRADING SCHEDULE

16. DISTRIBUTION STATEMENT (of this Report)

Approved for public release; distribution unlimited

17. DISTRIBUTION STATEMENT (of the abstract entered in Block 20, if different from Report)

18. SUPPLEMENTARY NOTES

19. KEY WORDS (Continue on reverse side if necessary and identify by block number)

Fatigue, Stress Relaxation, Anelastic Recovery

20. ABSTRACT (Continue on reverse side if necessary and identify by block number)

This thesis investigates stress relaxation, strain softening, strain hardening and anelastic behavior as potential recovery processes in 7075-T651 aluminum alloy. A series of tests were conducted utilizing specimens of 7075-T651 aluminum alloy as a representative aircraft structural material. The tests utilized both single and dual amplitude cyclic loading histories. The recovery mechanism felt to cause the observed stress decay was

represented as an exponential decay due to an anelastic strain recovery behavior. With the data obtained, stress decay to stabilization was discussed from the analyst's and the metallurgist's point of view. By having a through knowledge of the recovery process of the structural material, it will enable the structural analyst to develop better fatigue life prediction techniques.

An Investigation of the Recovery Processes in 7075-T651 Aluminum Responsible for a Stress Decay During Dynamic Loading Histories

by

Richard Allen Bentley
Lieutenant, United States Navy
B.S., Northrop Institute of Technology, 1970

Submitted in partial fulfillment of the
requirements for the degree of

MASTER OF SCIENCE IN AERONAUTICAL ENGINEERING

from the

NAVAL POSTGRADUATE SCHOOL
March 1977

ABSTRACT

This thesis investigates stress relaxation, strain softening, strain hardening and anelastic behavior as potential recovery processes in 7075-T651 aluminum alloy. A series of tests were conducted utilizing uniaxial specimens of 7075-T651 aluminum alloy as a representative aircraft structural material. The tests utilized both single and dual amplitude cyclic loading histories. The recovery mechanism felt to cause the observed stress decay was represented as an exponential decay due to an anelastic strain recovery behavior. With the data obtained, stress decay to stabilization was discussed from the analyst's and the metallurgist's point of view. By having a thorough knowledge of the recovery process of the structural material, it will enable the structural analyst to develop better fatigue life prediction techniques.

TABLE OF CONTENTS

LIST OF FIGURES

LIST OF SYMBOLS

σ	- Local stress
ϵ	- Total strain
ϵ_e	- Elastic strain
ϵ_p	- Plastic (creep) strain
σ_i	- Initial stress
t	- Time
E	- Elastic modulus
n'	- Emperical constant denoting creep behavior(varies between 0 and 1). Monotonic strain hardening exponent.
B	- Constant
K_T	- Elastic stress concentration factor(Geometeric)
S	- Nominal stress
$K_T S$	- Elastic notch stress
σ_R	- Residual stress
σ_{Req}	- Equilibrium value of the residual stress; that value that would exist had there been no previous history
$\sigma_{transient}$	- Nonequilibrium component of the residual stress that changes as a function of applied cycles
N_{ep}	- Equilibrium period, number of cycles for the local stresses to return approximately to equilibrium conditions following an overload
S_{OL}	- Difference between maximum working stress and peak overload stress
n,N	- Number of cycles at a given stress level
F_{ty}	- Tensile yield strength

I. INTRODUCTION

Of prime concern to the structural engineer is the requirement to be both mechanically efficient and cost effective in designing modern aircraft. A key element in satisfying this requirement is the method used for the fatigue life prediction of the airframe structure. Not only must sound structural theory be used, but also an understanding of cyclic material behavior is essential. To give the fatigue life prediction meaning, and greater accuracy, a fusion of the two theories must be effected. Only after this has been accomplished can damage theory be relied on to make the structure cost effective through a more realistic life span estimation. The paramount benefit from an accurate prediction capability would be safety of flight.

One question arising in the structural design of aircraft with respect to preventing fatigue failures is how the application of data obtained from tests of a few days duration can be properly applied to the prediction of aircraft life of several years. One commonly observed phenomenon in specimen testing is life lengthening due to compressive residual stresses, which occur as a result of plastic tensile deformation at a stress concentration (Ref. 1).

Two models of relaxation of residual stresses have

been postulated in recent years: one by an analyst and the other from a materials science point of view. Potter (Ref. 2), the analyst, proposed a model that the residual stress existing in a structure can be decomposed into two component parts at any given cycle in the structure's lifetime. One component, the equilibrium part, is that portion of the residual stress which would exist only because of the present nominal loading. For any given load spectrum, the equilibrium residual stress component could vary from cycle to cycle. The other component, the transient portion, represents the remaining amount of the residual stress and results from the preceding load history. The transient component of residual stress is responsible for load interaction and sequence effects.

The residual stress and strain are highly localized disturbances in an elastic continuum. Since they are disturbances, they are potentially unstable quantities and, given sufficient conditions, they will tend to be eliminated. Because of its variation from equilibrium, the transient component of the residual stress relaxation is a prime candidate for cycle-dependent relaxation. The tendency for such behavior is a function of the magnitude of the transient residual stress and the extent of the hysteresis in the local material. The greater the transient component and the greater the cyclic load plasticity, the greater will be the tendency for cyclic relaxation.

When cycle-dependent residual stress behavior occurs,

The transient residual stress decreases with cycles following the overload. Any reduction in the absolute value of the transient component will cause the rate of change in the residual stress simultaneously to decrease. This suggested to Potter a model where the residual stress decays exponentially. The residual stress response can be thought of as similar to a transient found in critically damped systems. Following an impulse, there is an asymptotic return to an equilibrium state. The overload triggers the impulse and controls its height.

The transient behavior of the residual stress was expressed in the exponential form given by

$$\sigma_{transient} = A \exp(bN) \ .$$

Potter proposed that when a transient response occurs following an overload, the local stress be described by

$$\sigma = K_T S + \sigma_{REQ} + \sigma_R - \sigma_{REQ} \exp (N/N_{EP}) \ln 0.1 \ .$$

For all the fatigue tests that Potter conducted concerning load interaction effects, non-zero equilibrium residual stresses existed during the constant amplitude cycling. Because of this, the transient component of the residual stress at N=0 is equal to the negative of the applied overload stress. Therefore,

$$\sigma = K_T S + \sigma_{REQ} - K_T S_{OL} \exp (N/N_{EP}) \ln 0.1$$

Using this model of the local stress behavior, it is pos-

sible to explain the fatigue behavior of notched structures subjected to periodic overloads. The term $\exp(N/N_{EP})$ as defined by Potter will provide mathematical modeling of a cyclic dependent stress relaxation.

Another proposed model, from the metallurgical point of view, has been developed at the University of Illinios, Department of Theoretical and Applied Mechanics by Jhansale (Ref. 3). The transient and steady state stress-strain hysteresis behavior of several structural metals were analyzed in this study, and of main interest was the testing of 7075-T6 aluminum. The study showed that a stress parameter, defined as the "Yield Range Increment," uniquely denoted various transient phenomena including cyclic hardening, softening, relaxation, creep and the steady state cyclic stress-strain behavior. The yield range increment is a history dependent stress parameter. By its variation or constancy it quantitatively denotes the cyclically dependent transient phenomena of the material in question. All transient and steady state hysteresis branches of a given material appear to be identical "elastic" parts are deleted. A mathematical model incorporating the "Yield Range Increment" is illustrated in (Fig. 1).

From the discussion of residual stress relaxation in these models there arises the question as to what is the actual process by which the stress decays as a function of time. The analyst's point of view suggests that "relaxation" implies a mathematical process of stress decay in contrast to

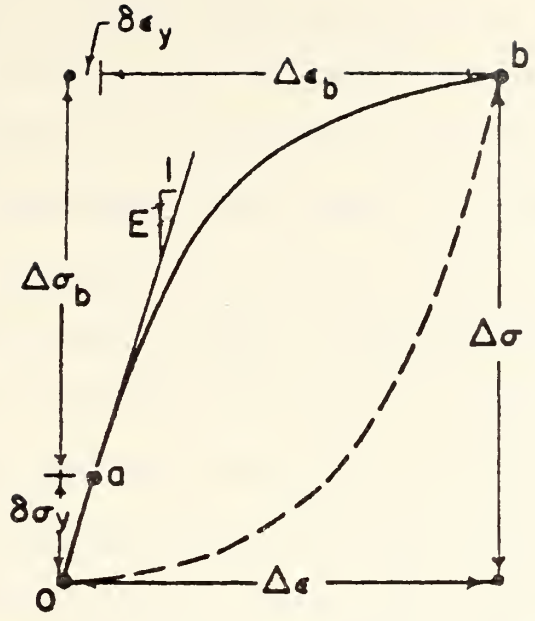

Portion oa is "Yield Range Increment".
Portion ab is "Basic Hysteresis Curve".

Mathematical Model

$$\Delta\epsilon = \Delta\sigma/E + \left(\frac{\Delta\sigma-\delta\sigma_y}{K}\right)^{1/n} \quad \text{for } \Delta\sigma > \delta\sigma_y$$

$$\Delta\epsilon = \Delta\sigma/E \quad \text{for } \Delta\sigma \leq \delta\sigma_y$$

E, K and n are history independent material parameters.

$\delta\sigma_y$ is the history dependent "elastic" parameter.

Figure 1

A mathematical model incorporating the "Yield Range Increment"

the metallurgical definition of the term relaxation. It is felt that a better understanding of the recovery process taking place during the loading history would make the material behavior more appropriately adapted to the fatigue damage calculation. The process, or processes, responsible for such decay are varied and difficult to isolate in an experimental test. Other mechanisms besides relaxation that are felt to have an influence on the stress decay are strain hardening, strain softening, and anelastic strain recovery.

Investigation into cyclically dependent stress recovery is the main focus of this thesis, and an effort to observe the stress recovery trends over a number of cyclic loading histories will be conducted. An effort will also be made to establish a better physical representation of the actual stress decay process taking place. The term relaxation is used interchangibly by the analyst to mean an exponential decay in stress as a function of cycle or time. In the text of this thesis the term relaxation will be used mainly as a metallurgical term unless used in connection with the mathematical description of the experimental data. The relaxation rate coefficient listed in the tabular data will be used to describe this decay rate behavior.

II. FOUR RECOVERY MECHANISMS OF INTEREST

In recent years, the significance of fatigue under large strain amplitudes ("low cycle" fatigue) has resulted in considerable interest in the cyclic behavior of material in the plastic range. The Manson-Coffin law for predicting failure due to strain cycling is the most widely known product of this interest.

Although strain cycling is an important mode of plastic deformation of materials, only limited work has been reported on the macroscopic stress-strain behavior during strain cycling. Several investigators have examined the behavior of the total stress range of the cyclic hysteresis loop as a function of total strain range and cyclic exposure and have obtain measures of the energy expenditure per cycle (Ref. 4). This energy expenditue per cycle is possible through the recovery mechanisms taking place in the material. The four recovery mechanisms that concern this investigation are discussed to explain the significance of their behavior during the cyclic loading histories utilized.

In this section the differences and similarities of the possible recovery phenomena taking place will be discussed. The recovery behavior thought to have a major role in the stress decay process may be a combined action of relaxation, strain hardening, strain softening and anelastic structural behavior. From the experiments conducted in support of this thesis, anelastic behavior is thought to have the major role

in stress decay during cyclic histories.

To discuss stress relaxation, the creep phenomenon has to be coupled to the relaxation behavior. Stress relaxation is thought of in context of fixed strain, while creep is thought of as occurring under fixed stress. The time-dependent relationship is very similar. Following Dieter (Ref. 5), let us consider a tension specimen which is subjected to a total strain, ϵ, at an elevated temperature where creep can occur.

$$\epsilon = \epsilon_e + \epsilon_p = \frac{\sigma}{E} + \epsilon_p$$

As the material "creeps" (lengthens) the total strain can only remain constant if the elastic strain decreases. Differentiating the above equation with respect to time, and remembering that $d\epsilon / dt = 0$,

$$d\epsilon_e / dt = - d\epsilon_p / dt$$

But $\epsilon_e = \frac{\sigma}{E}$, and if $d\epsilon_p / dt = B\sigma^{n'}$

$$\frac{1}{E} \frac{d\sigma}{dt} = - B\sigma^{n'}$$

Integrating,

$$\int \frac{d\sigma}{\sigma^n}, = -BE \int dt$$

$$- \frac{1}{(n'-1)\sigma^{n'-1}} = -BEt + C$$

At t=0, $\sigma = \sigma_i$, so that

$$C = - \frac{1}{(n'-1)\sigma_i^{n'-1}}$$

Therefore, the relation between stress and time in stress relaxation is given by

$$\frac{1}{\sigma^{n'-1}} = \frac{1}{\sigma_i^{n'-1}} + BE(n'-1)t \quad .$$

This brief examination shows that stress relaxation and creep are, in fact, related. The initial rate of decrease of stress is high, but it levels off because as the stress level decreases, the creep rate decreases.

The most common load relaxation test for metals consists of loading a specimen in tension or compression in a tensile testing machine to some predetermined load level, then stopping the crosshead motion, and subsequently recording the load as a function of time. The resultant load-time record is dependent both on the plastic properties of the specimen and the testing machine, which is negligible in the Material Testing System machine. This is predominantly a static relaxation type of test. Of prime concern, though, is the cyclic relaxation behavior.

Present formulations to describe the cyclically dependent phenomena of transient hardening, softening, relaxation and creep are schematically illustrated in (Fig. 2).

In discussing the phenomenon of strain softening an understanding of strain hardening is necessary, as illustrated in (Fig. 2a and 2b). Strain hardening is caused by dislocations interacting with each other and with barriers, which impede their motion through the crystal lattice. Hardening due to dislocation interactions is a complicated problem because it involves large groups of dislocations, and it is difficult

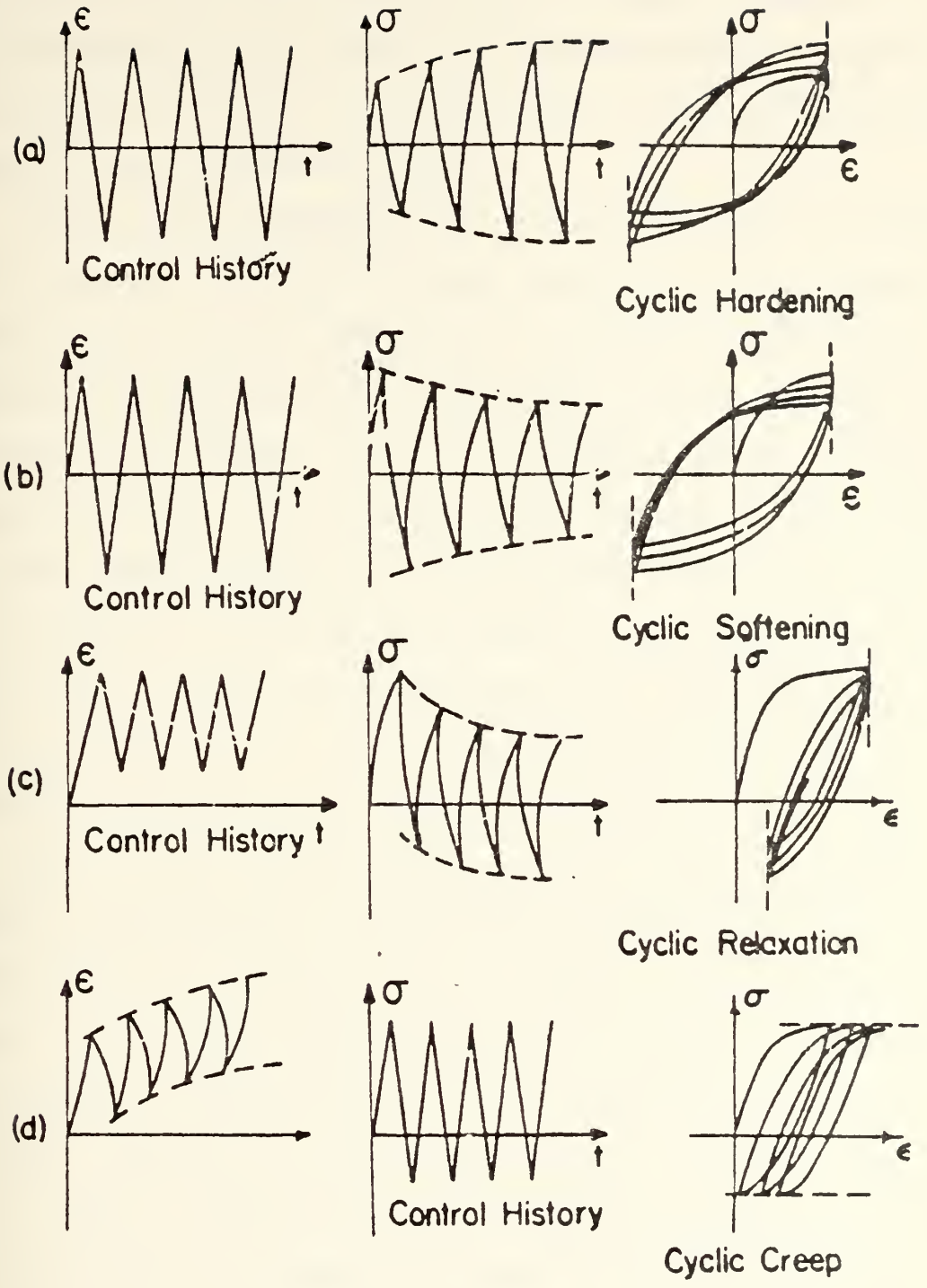

Fig. 2 Schematic Illustrations of Cyclic Transient Phenomena

to specify the group behavior in a simple mathematical way. It is known that the number of dislocations in a crystal increases with strain over the number of dislocations present in the unstrained lattice.

While cycle dependent mean stress relaxation is denoted by a decrease in absolute mean stress with cycle under constant strain cycling situations, as shown in Fig. 2(c), cyclic dependent creep is manifested as an increase in the absolute mean strain with cycles under constant stress cycling situations, as illustrated in Fig. 2(d). While there is some physical basis for the concepts used for hardening or softening and hysteresis response, the basis for relaxation and creep is essentially mathematical. These approaches have been necessitated by a lack of complete understanding of the material response under cyclic situations.

One of the earliest dislocation concepts to explain strain hardening was the idea that dislocations pile up on slip planes at barriers in the crystal. The pile-ups produce a back stress which opposes the applied stress on the slip plane. Upon reloading in the opposite direction, the lattice yields at a lower shear stress than when first loaded. This is because the back stress developed as a result of dislocations piling up at barriers during the first loading cycle is aiding dislocation movement when the direction of slip is reversed. When the slip direction is reversed, dislocations of opposite sign could be produced at the same sources that produced the dislocations responsible for strain in the first direction. Since dislocations

of opposite sign attract and annihilate each other, the net effect would be a further softening of the lattice structure. This reverse of dislocation movement is called the Bauschinger effect (Ref. 5). While all metals exhibit this effect, it is of varying magnitudes in each.

Another area of plastic strain recovery, or stabilization, is the phenomenon of anelastic behavior. If a metal is strained to point A, (Fig. 3), Hookes law is followed up to some yield stress σ_o . Beyond σ_o, the metal deforms plastically. Most metals strain-harden in this region, so that increases in strain require values of stress than the initial yield stress. However, unlike the situation in the elastic region, the stress and strain are not related by a constant of proportionality. If the metal is strained to point A, when the load is released the total strain will immediately decrease from ϵ_1 to ϵ_2 by an amount σ_A / E. The strain decrease $\epsilon_1 - \epsilon_2$ is the recoverable elastic strain. However, the strain remaining is not all permanent plastic strain. Depending upon the metal and the temperature, a small amount of the plastic strain $\epsilon_2 - \epsilon_3$ will disappear with time. This is known as anelatic behavior.

In this work a qualitative analysis is made of the details of the stress-strain behavior in 7075-T651 aluminum. Particular interest has been devoted to time dependent anelastic behavior and strain hardening effects during cyclic loading.

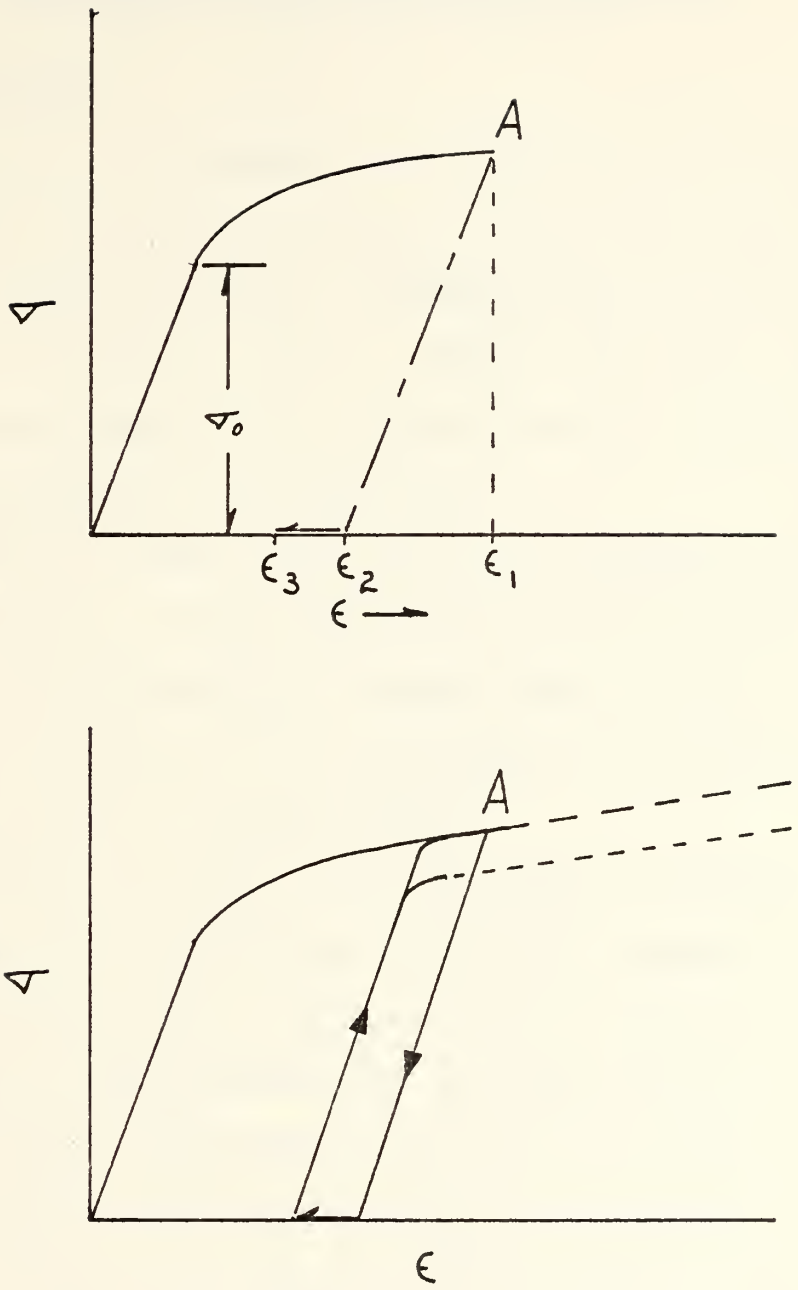

Figure 3

An illustration of Anelastic behavior

III. STRESS STABILIZATION DATA ON UNIAXIAL SPECIMENS OF 7075-T651 ALUMINUM

A. INTRODUCTION

To provide data relating to the stress recovery behavior taking place in the test material, a series of tests were conducted utilizing uniaxial specimens made of 7075-T651, illustrated in (Figs. 4 and 5). These tests were performed to discover and quantify the actual recovery mechanism involved during cyclic load histories.

Relaxation as used by the analyst to explain stress decay was investigated. It was felt that the tests conducted revealed the true mechanism of substructural recovery and explained why there may be a misnaming of the stress relaxation behavior that is taking place.

The material specimens were subjected to various fixed strain range cyclic histories. The first sequence included a look at the hysteresis behavior and the influence of repeated cyclic loading periods on the same uniaxial specimen. The second series subjected the material to single and dual amplitude cyclic loading histories to investigate the cyclic relaxation behavior at various strain ranges. The third sequence included tests to demonstrate the possible anelastic behavior to account for the observed cyclic stress decay. The anelastic property of 7075-T651 is focused on as a main source of plastic strain recovery, accounting for a time dependent stress decay. The individual tests will be described

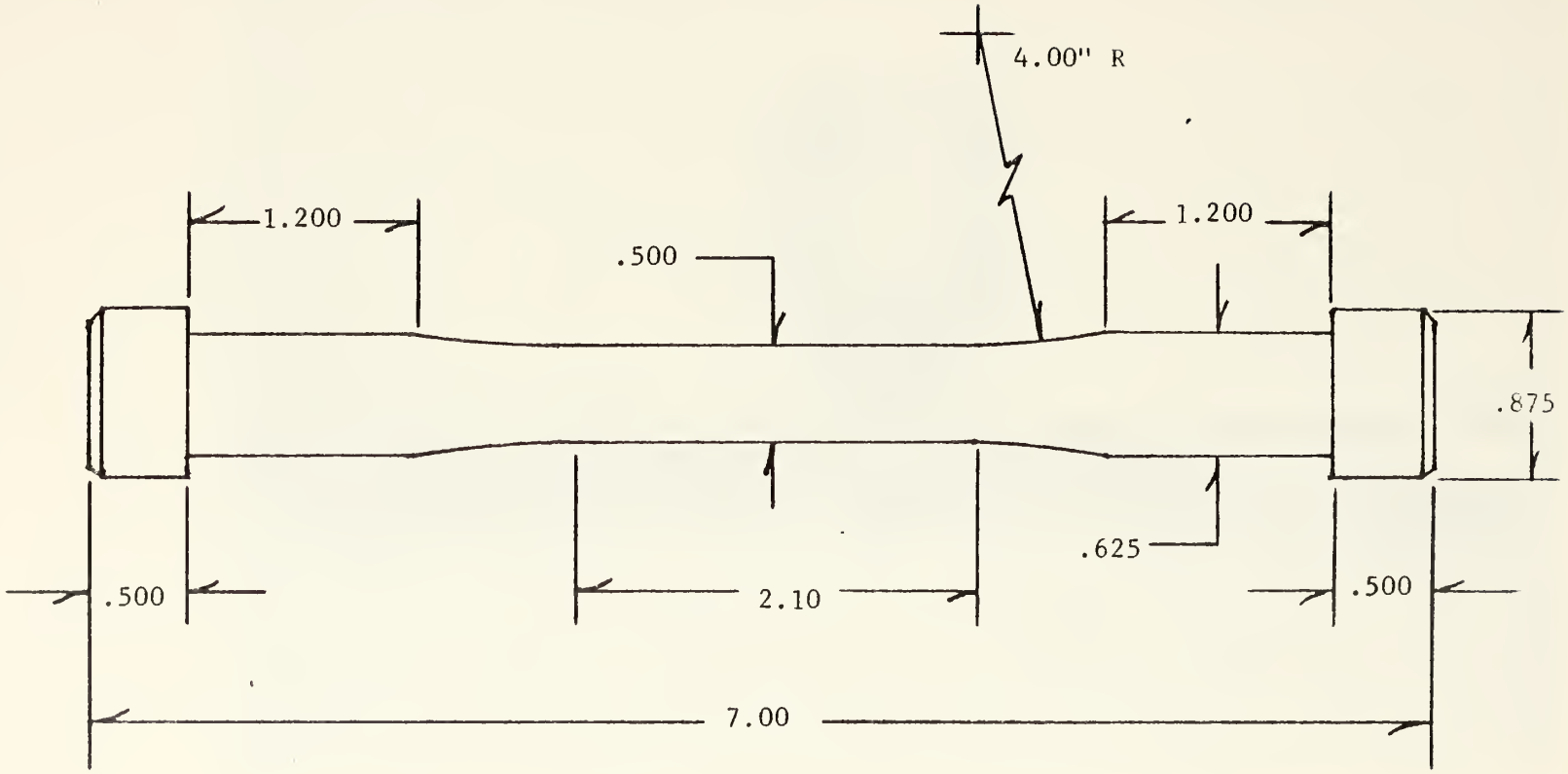

Figure 4
Uniaxial Specimen of 7075-T651

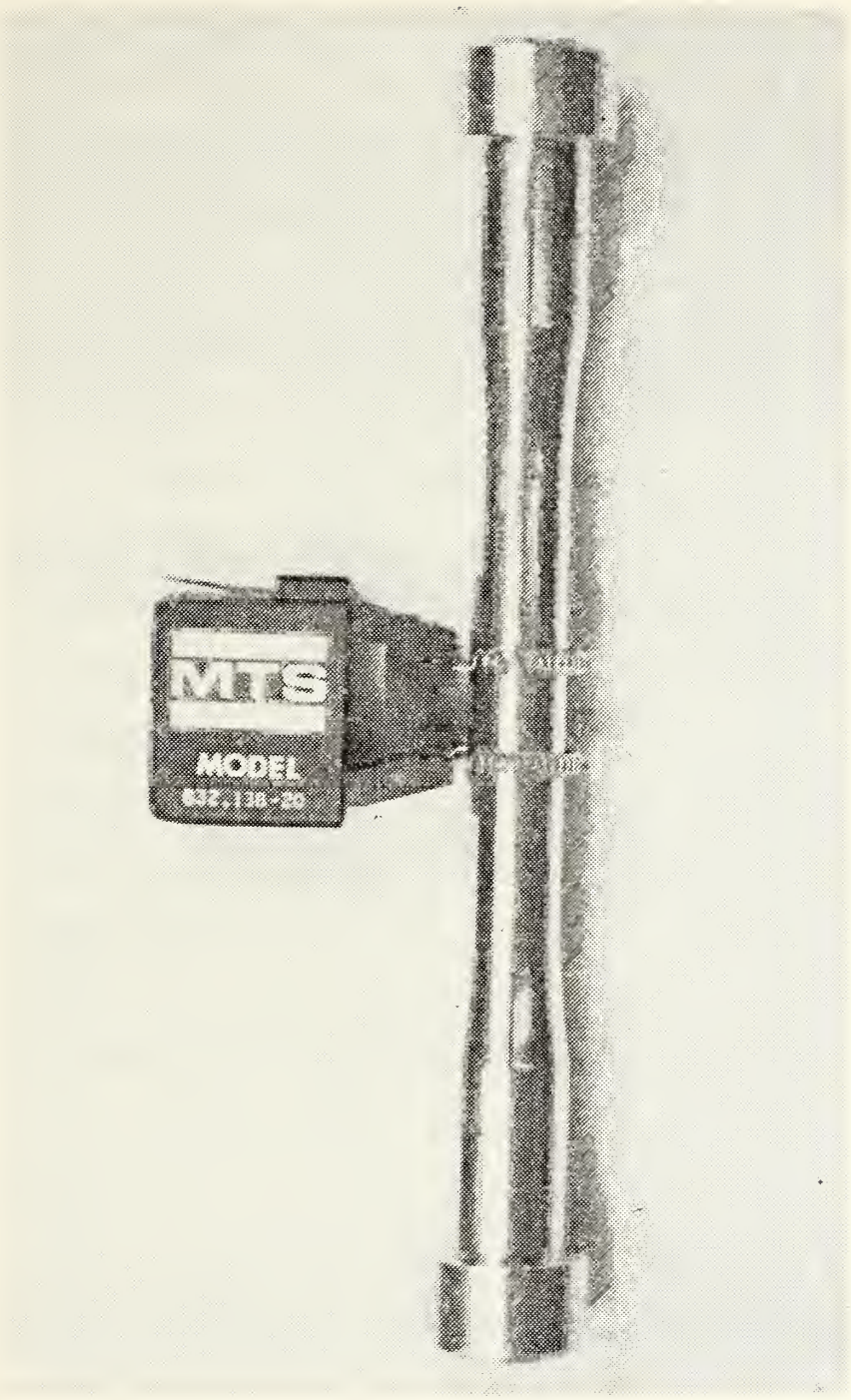

Figure 5

Photo of uniaxial specimen with
MTS Extensometer attached

in detail later in this section.

The data obtained from the uniaxial specimens will be considered indicative of the properties of the structural material around a stress concentration that will force the structure into the plastic range. Considering this aspect, results of tests on these uniaxial specimens would not be confined to a single geometry.

The testing of the uniaxial specimens was done using an MTS Systems Corporation Series 810 closed loop, servo-controlled testing system (Figs. 6 and 7). The system was driven under strain control on all tests by an internal function generator for the single amplitude tests, and driven by an Electronics Associates Incorporated TR-20 analog computer on the dual amplitude tests. All strain and load output voltages from the specimen during testing were recorded on a Hewlett-Packard dual trace strip chart recorder and a Hewlett-Packard X-Y recorder.

The uniaxial specimens used in the tests were machined from 7075-T651 aluminum bar stock in accordance withASTM recommendations (Ref. 6). The physical characteristics of the specimen may be seen in (Figs. 4 and 5). The alloy make up consists of 1.6% copper, 2.5% magnesium, 5.6% zinc, .3% chromium with a .2% offset yield strength of 72 KSI and an ultimate strength of 82 KSI. 7075-T651 aluminum alloy is extensively used in high strength roles in aircraft structures requiring a high fracture toughness. The T651 heat treat has the greatest plane stress and plane strain fracture toughness of any similar heat treated aluminum alloy.

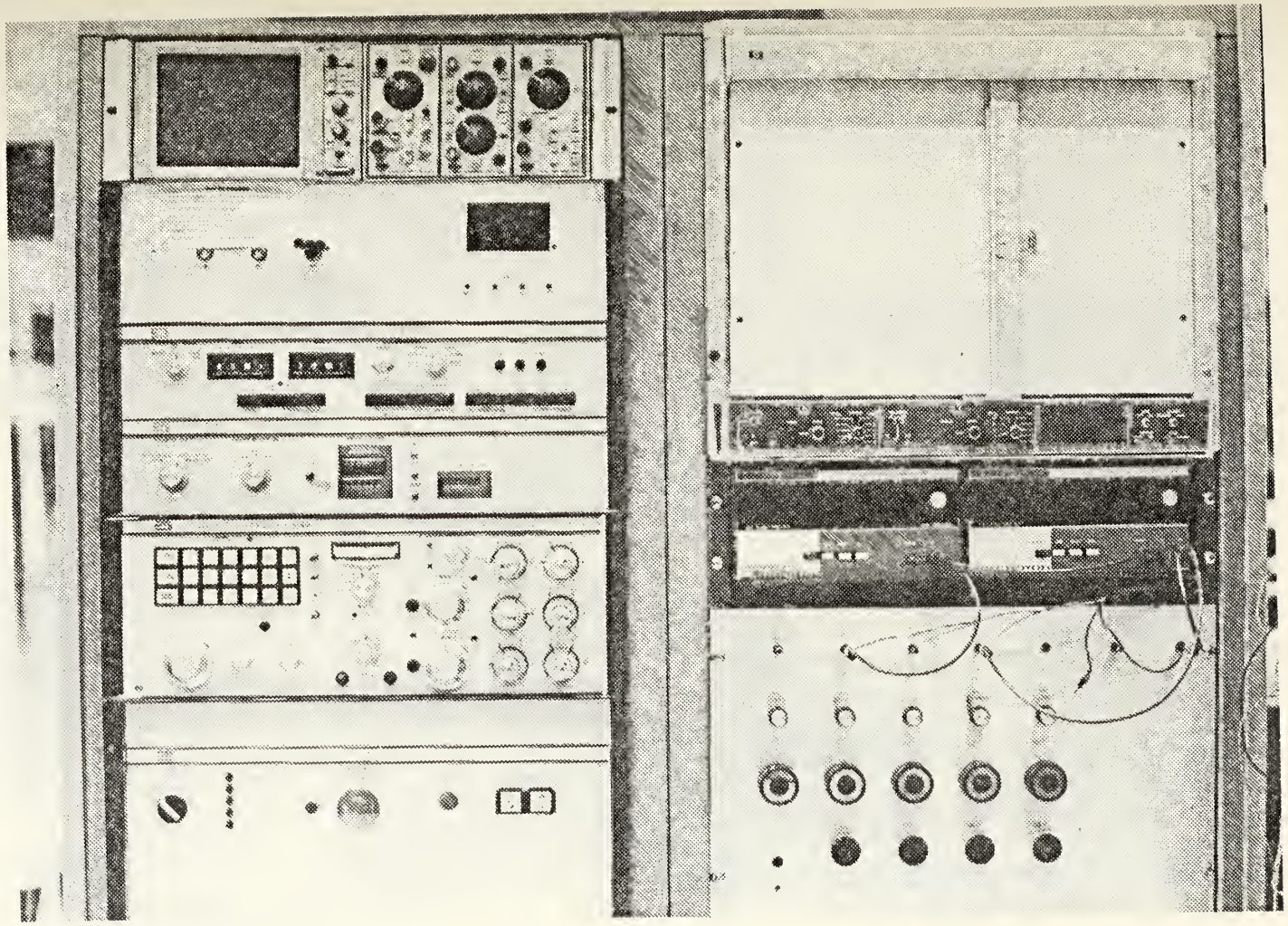

Figure 6

Photo of MTS System

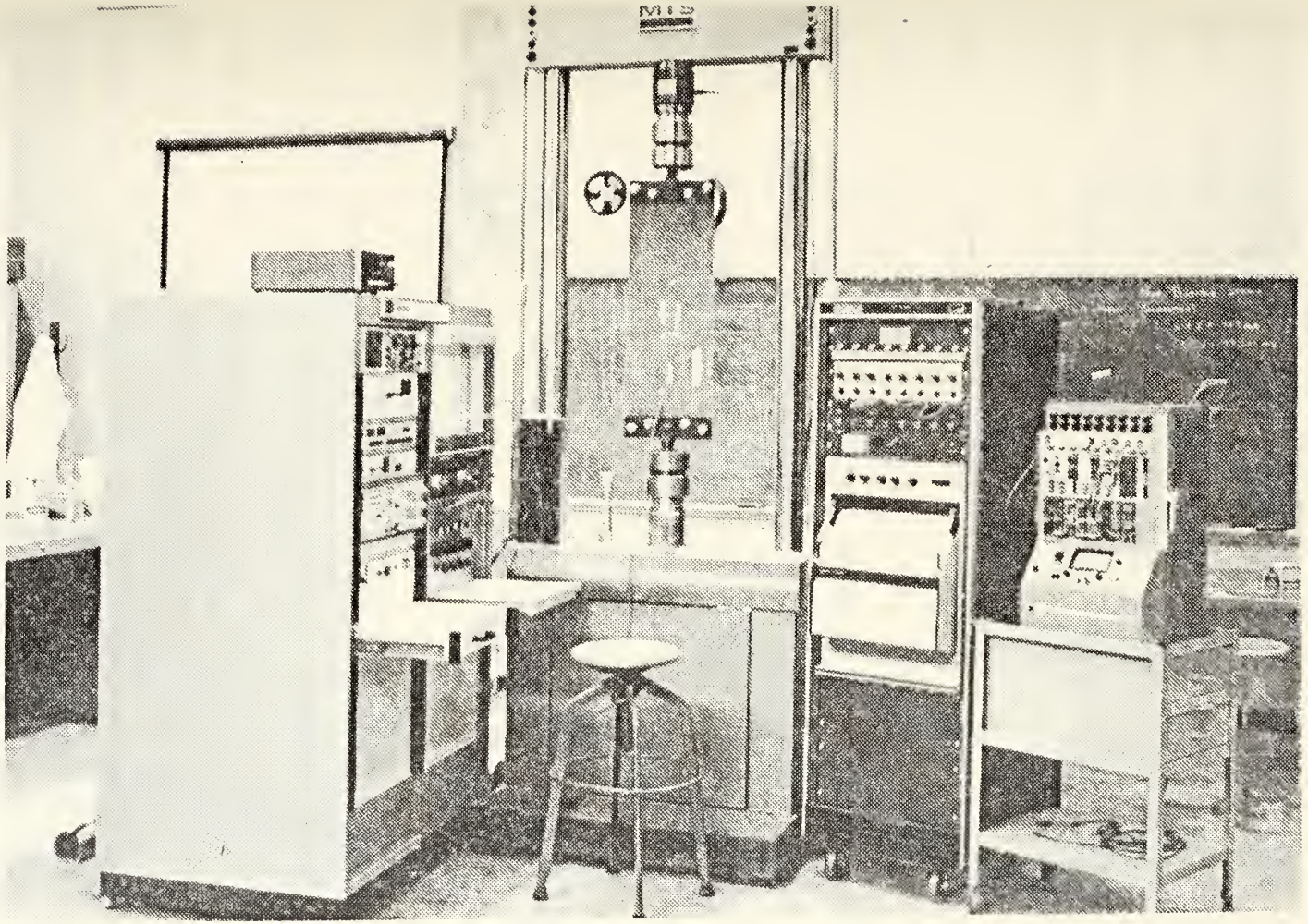

Figure 7

Photo of MTS System

The extensometer used was manufactured by the MTS Systems Corporation (Ref. 7). The physical specifications can be seen in (Fig. 8). The actual attachment to the specimen can be observed in (Fig.5). All extensometers are certified by MTS Systems Corporation, and all calibration done at room temperature. The extensometers are calibrated in four strain ranges. Several models have such small full scale displacement in the last one or two ranges that calibrators are not sensitive enough to mechanically check these ranges. The strain ranges equal to or greater than $\pm$ .010-inch are mechanically calibrated, but for ranges less than $\pm$ .010-inch the end points are electronically calibrated. This is possible because the ranges are proportional to each other, which allows the other points to be determined. The lowest strain range on the MTS System was used during the tests; therefore, the extensometer was electronically calibrated using a wheatstone bridge. The corresponding input voltage is graphically represented in (Fig. 9 and Table 1).

At the beginning of each test, the MTS extensometer was attached to the unstressed specimen at zero load cell voltage indicated by a load cell voltage output of zero. The extensometer output voltage was then zeroed through the strain transducer controller on the MTS system. It is felt that an accuracy of $\pm$ 0.1 mv was attained in this initial process. This initial zeroing procedure was done in load control. There was no significant voltage change noted during transition to the strain control mode for the execution of the test history.

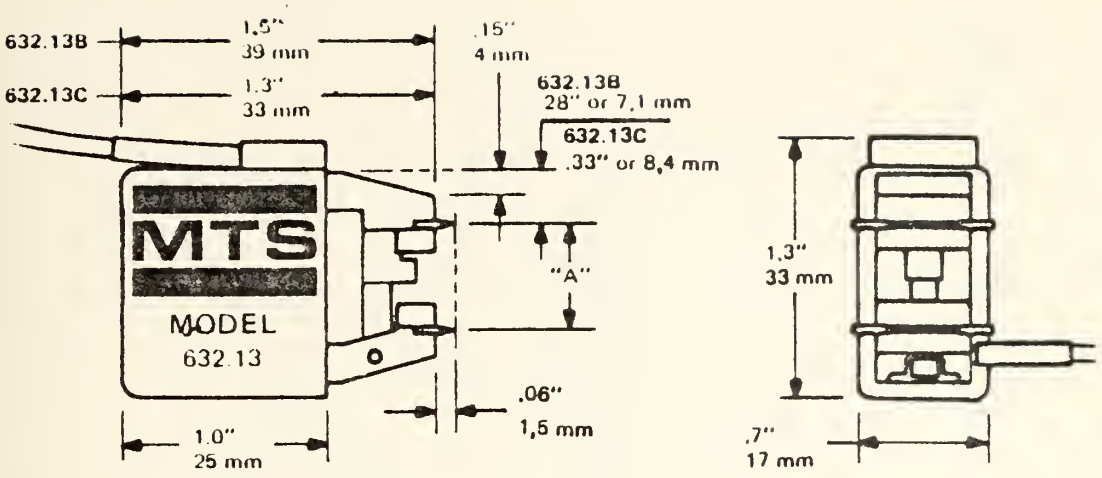

MODEL	English Metric	632.13B-20 632.13C-20
Gage Length (Dimension A)		.500" ± .002 10mm
Max. Range of Travel (Strain)**		±.150 strain
Linearity***		0.25% of range
Ranges where extensometer may be calibrated to ASTM	Class B1 Class C	0 to .04 0 to .15
Max. Hysteresis		0.1% of range
Temperature Range		-115° to 250°F
Immersibility		Yes*
Max. operating frequency with negligible distortion		100 Hz
Weight (less cable and connector)		22 gm
Operating force full scale	English Metric	35 gm 45 gm
Recommended calibrated ranges for 10v full scale output from MTS transducer conditioner****		±.20 ±.10 strain ±.04 ±.02

Figure 8

MTS Extensometer Model 632.13 Specifications

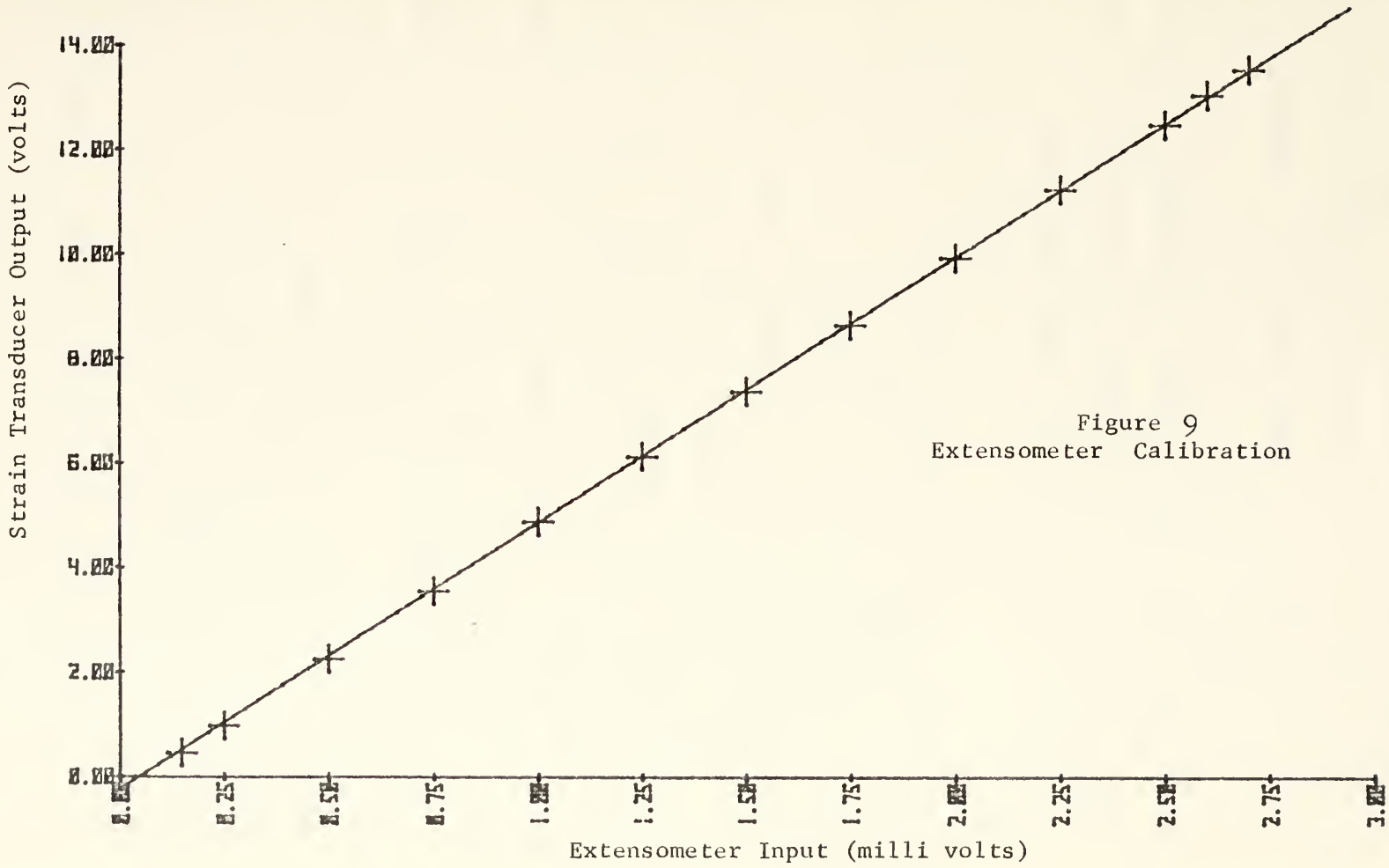

Figure 9
Extensometer Calibration

B. SINGLE AMPLITUDE CYCLIC LOADING TESTS

1. Description of Test

In this test, the presence of stress relaxation behavior in the uniaxial specimens of 7075-T651 aluminum was investigated. The data compare the effect of the magnitude of the initial strain loading on the rate of stress decay of different loading histories. The single amplitude data were also compared with the stress decay behavior of a dual amplitude cyclic history following a similar initial loading.

The tests were conducted with an initial strain level that was identical in all tests of this sequence. This was done to show the dependence of the relaxation behavior on the initial strain experienced by the material in question. After the initial strain imparted to the uniaxial specimen, each test sequence was conducted by varying the strain range between a minimum and a maximum level for 150 cycles. An example of the load history is illustrated in Fig. 10. The cycle frequency was 0.12 HZ. This frequency was well within the capabilities of the strip recorder and the X-Y plotter. It was felt that a manual record of the load history voltage on each cycle from a digital voltmeter was more accurate than relying totally on data retrieval from the strip recorder alone. The strip recorder was used as a backup for peak load and strain applications during the cyclic history.

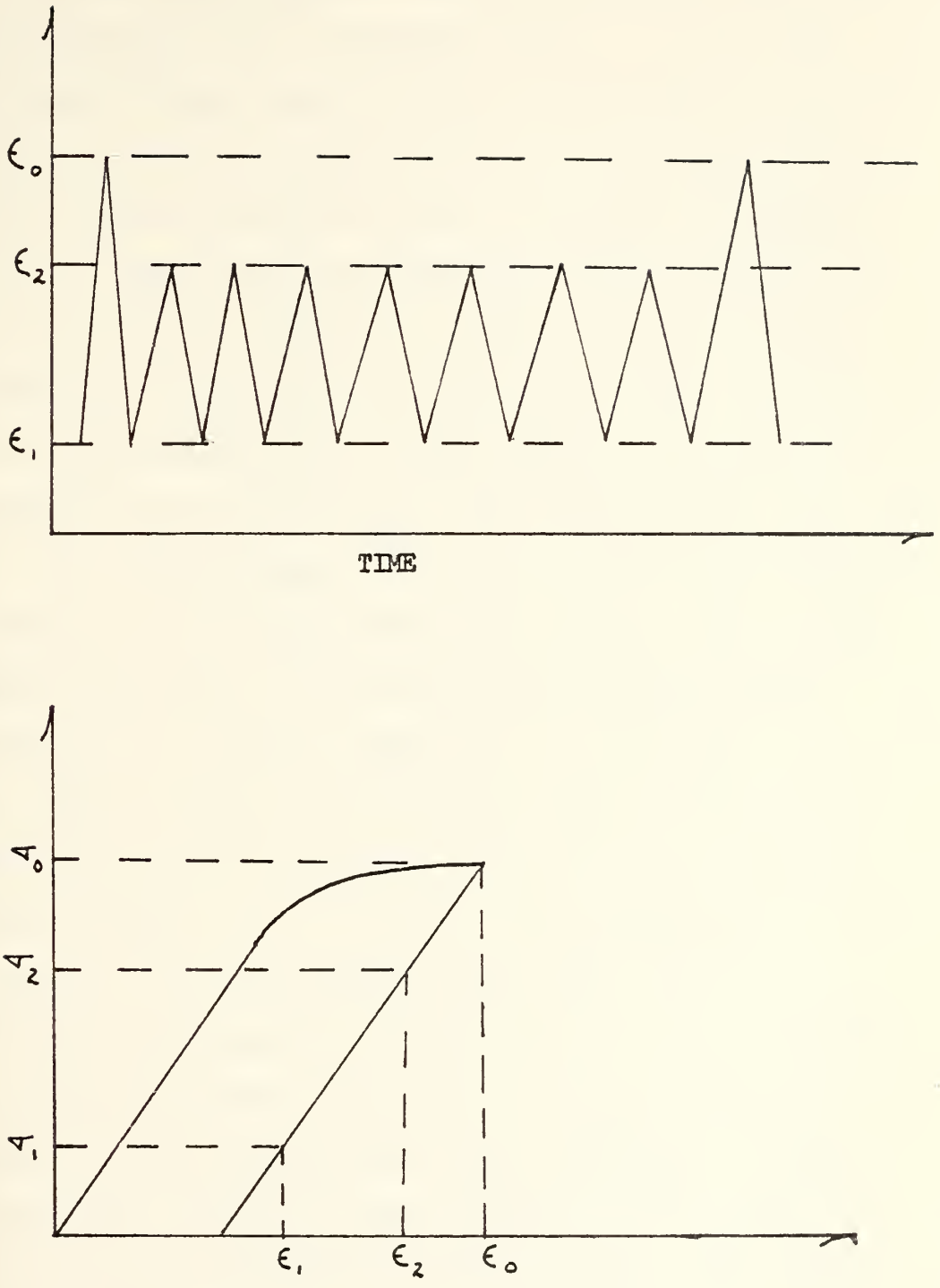

Figure 10

Illustration of single amplitude cyclic load history

2. Test Results

In this test sequence two test specimens were run during each phase to get comparable data. In all tests cycled between fixed strain limits in the elastic range of the specimen little recovery was noted. By trying the exponential stress relation as used in Potter's relaxation model, $\sigma = \sigma_o \exp(-bN)$, the b exponent value was plotted as a function of cycle number. A rapid initial decrease to a stabilized relaxation rate was noted. The transient behavior to stabilization is illustrated in the plots of the relaxation rate coefficient verse cycle number (Figs. 11, 12, and 13). These figures indicate that the most significant changes in the stress range occur within 16% to 20% of specimen test life. The tabular data taken during these tests can be seen in Tables 10, 11, and 12.

When these relaxation datum were curve fitted using an exponential curve fit routine, they exhibited a poor correlation factor of $r^2 = 0.303$. As illustrated in Figs. 14 and 15 the log stress verse cycle number is represented by an apparent straight line. Due to the fact that the scale supresses the data, it showed a misrepresentation of a true exponential decay behavior. As seen from the actual relaxation rate behavior, b, it does not conform to a true exponential decay behavior. The value of b, as seen in Figs. 11, 12, and 13, is not a constant throughout the decay to stabilization. The decay behavior acts like a damped system with an initial impulse function represented by the initial strain loading.

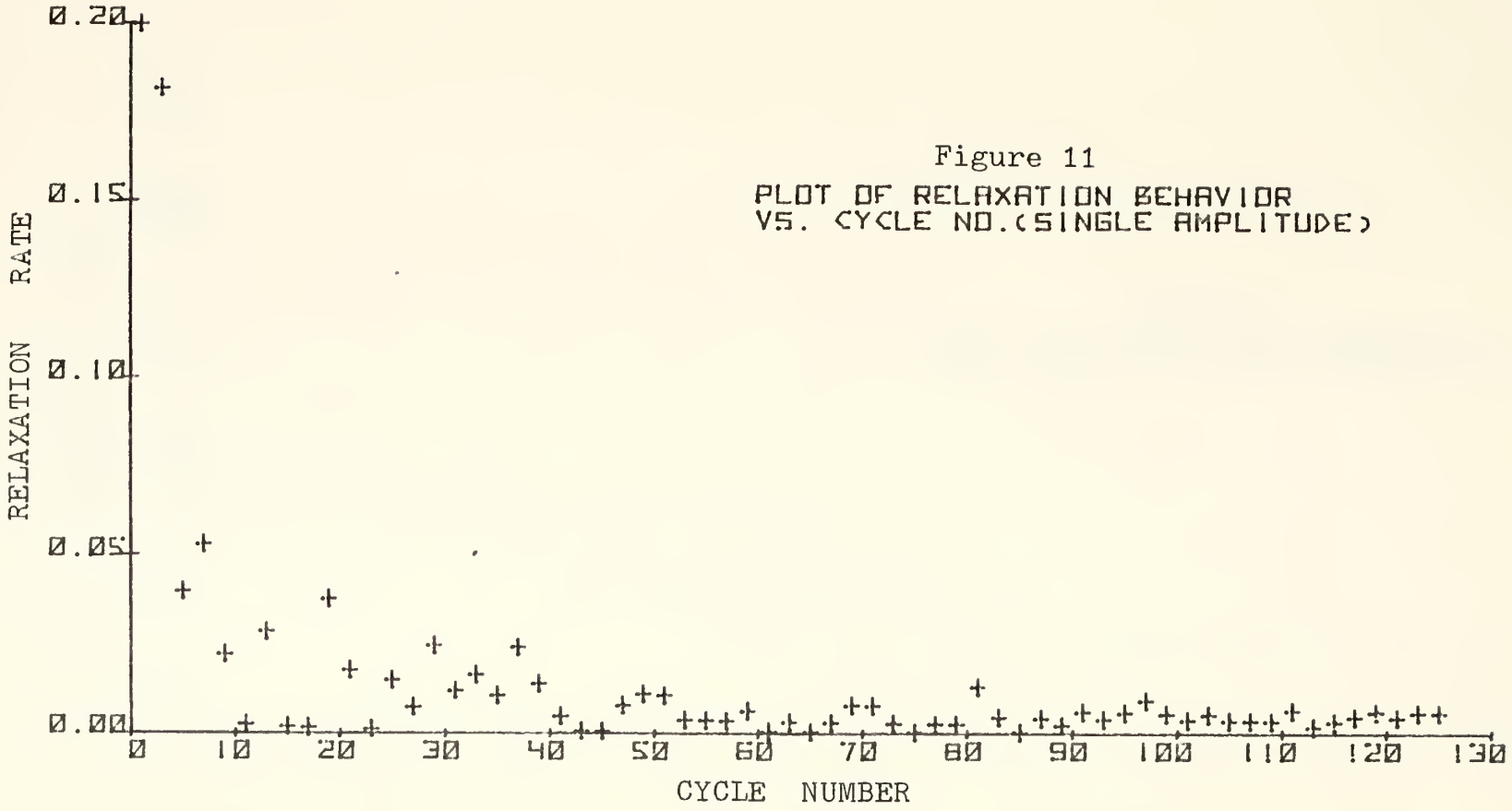

Figure 11
PLOT OF RELAXATION BEHAVIOR
VS. CYCLE NO.(SINGLE AMPLITUDE)

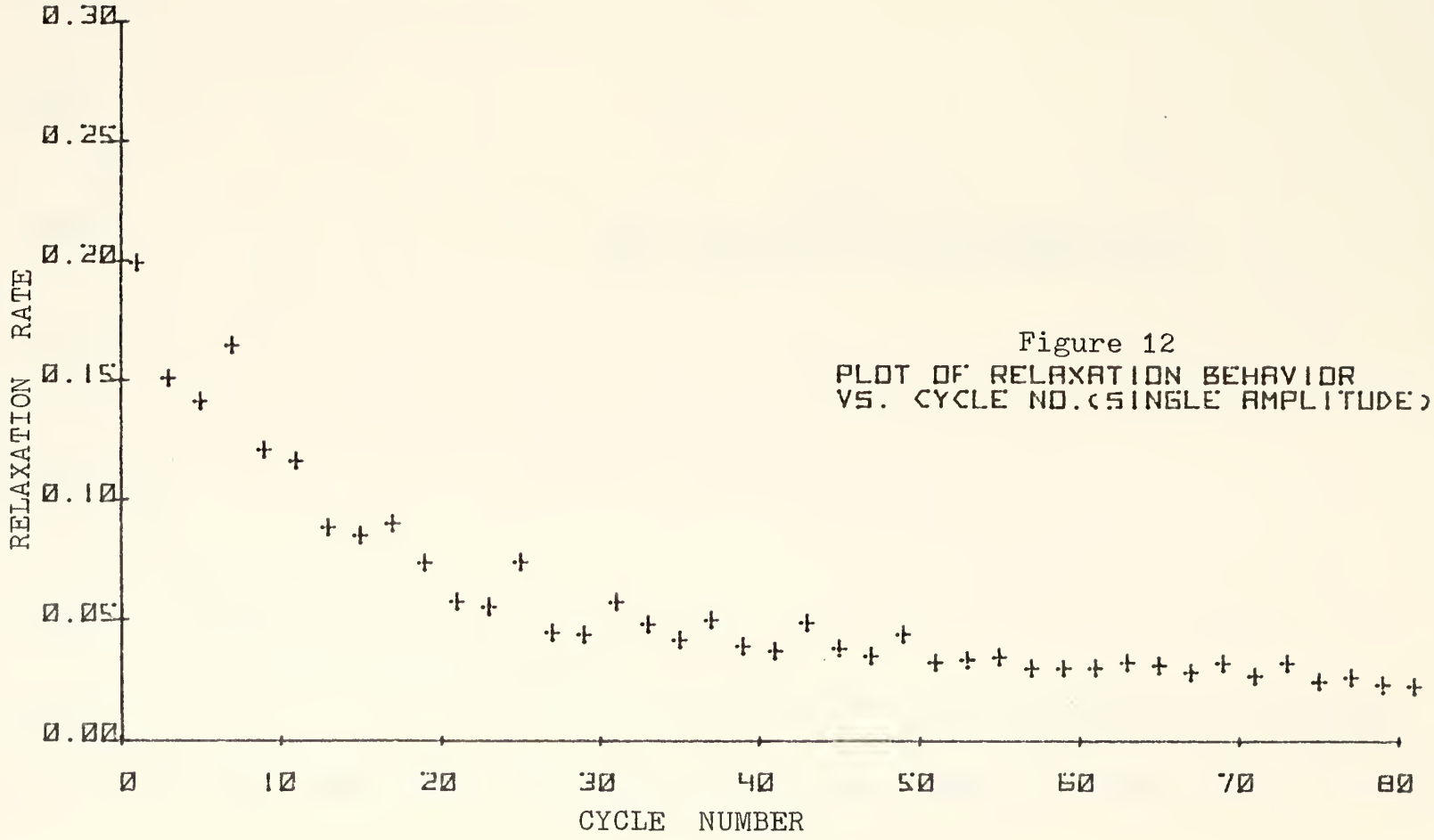

Figure 12
PLOT OF RELAXATION BEHAVIOR
VS. CYCLE NO.(SINGLE AMPLITUDE)

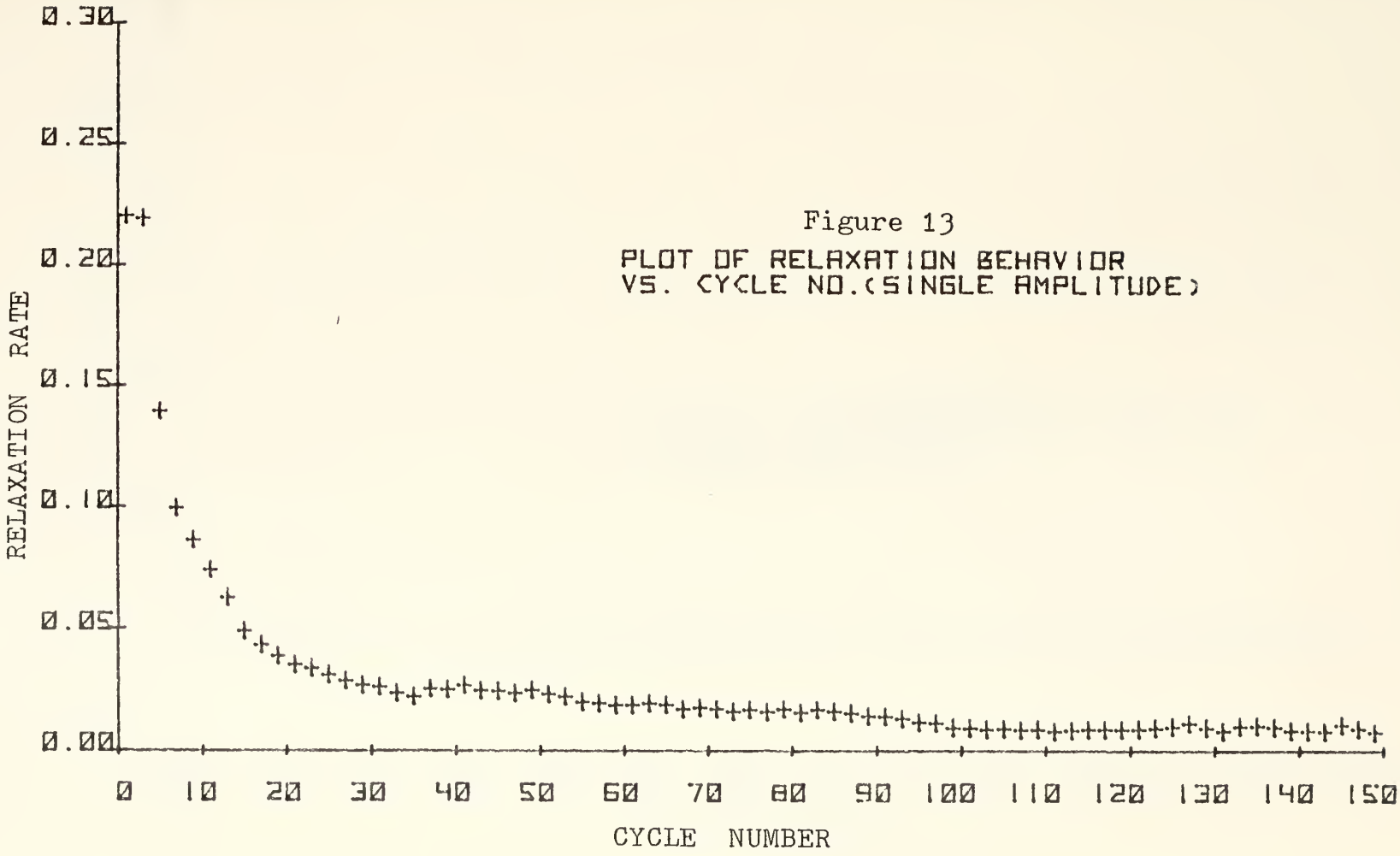

Figure 13
PLOT OF RELAXATION BEHAVIOR
VS. CYCLE NO.(SINGLE AMPLITUDE)

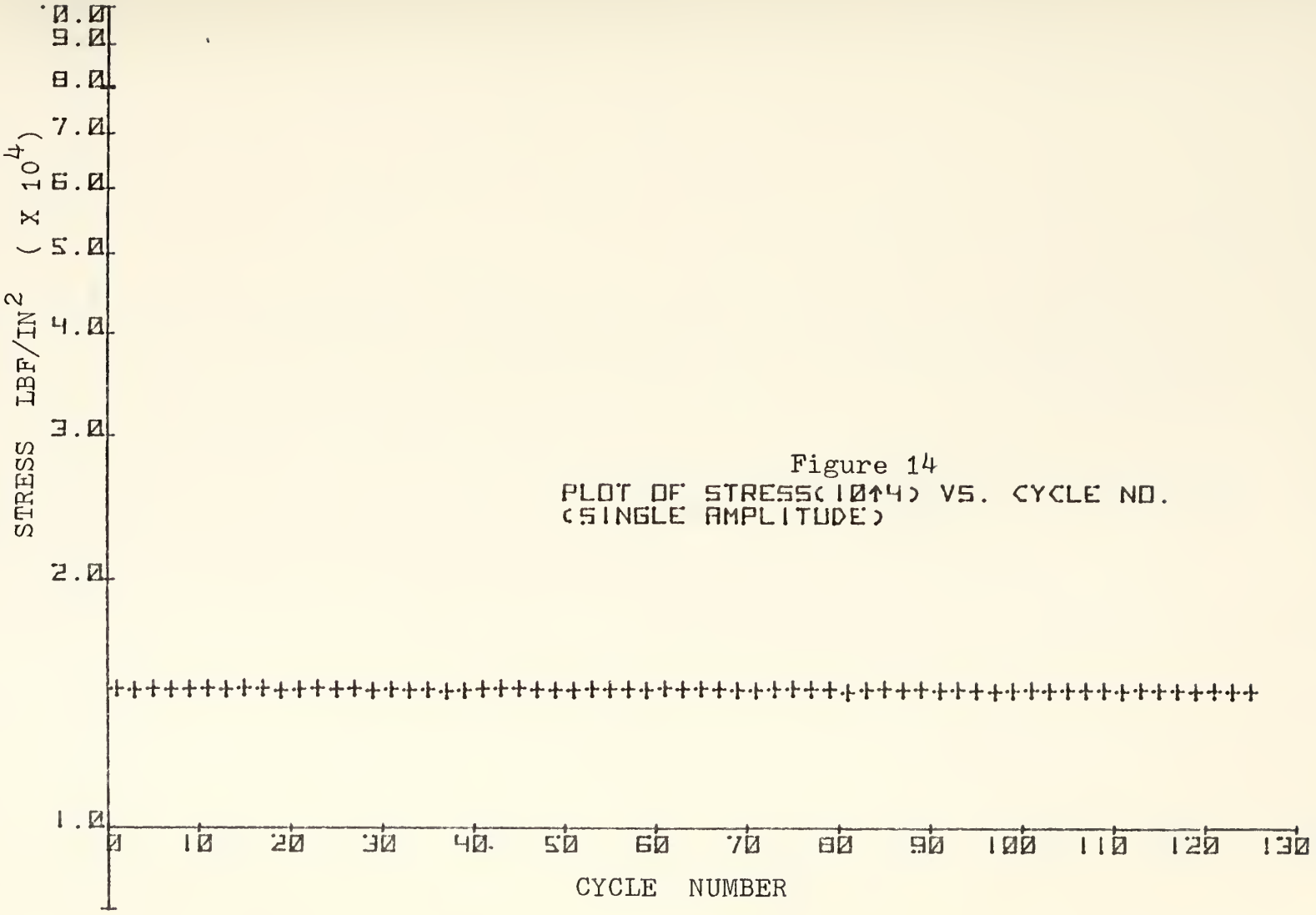

Figure 14
PLOT OF STRESS(10↑4) VS. CYCLE NO.
(SINGLE AMPLITUDE)

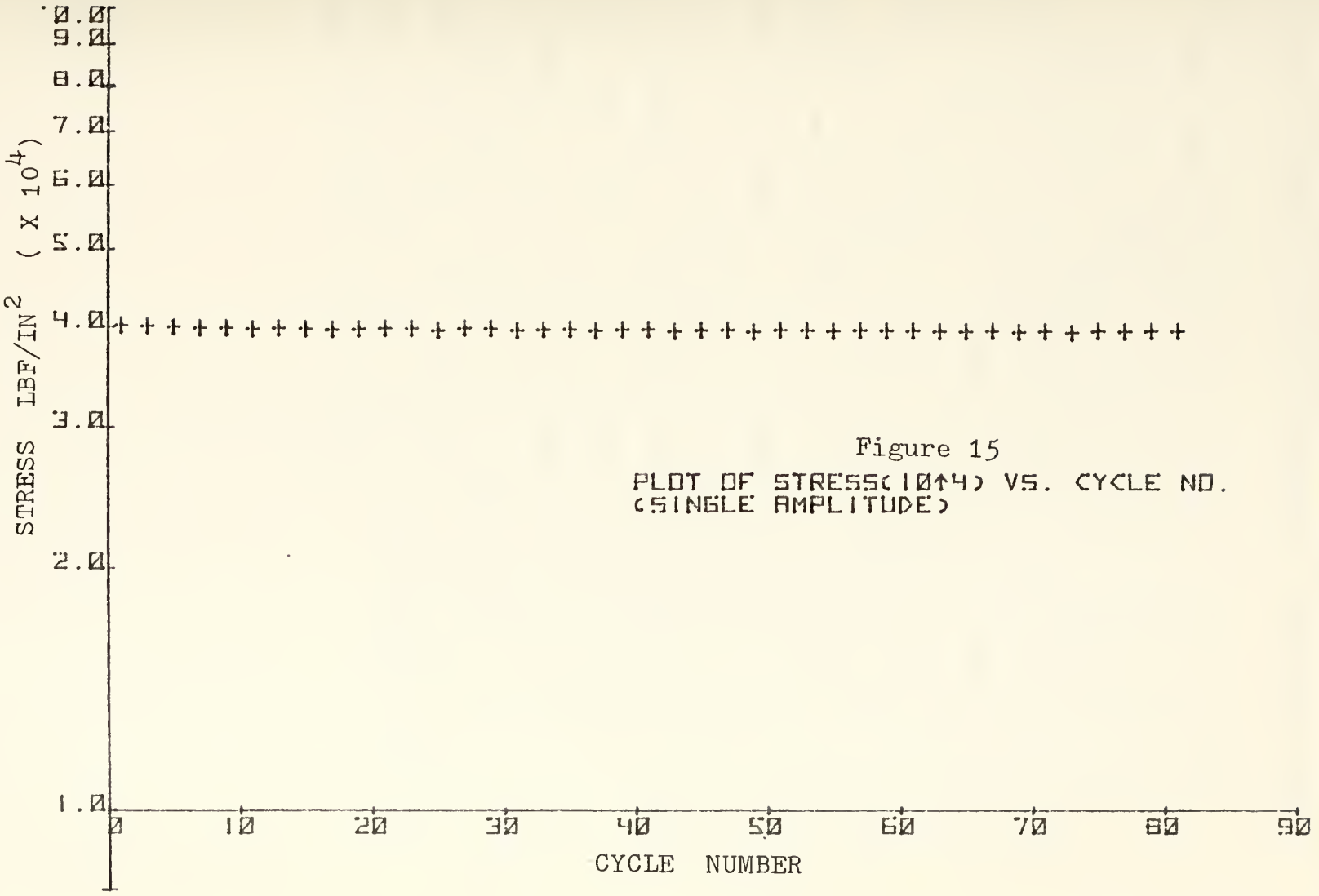

Figure 15
PLOT OF STRESS(10↑4) VS. CYCLE NO.
(SINGLE AMPLITUDE)

The recovery observed when treated by the exponential modeling reduced to the following for the three strain ranges.

Low strain range: $\sigma = 14{,}900 \exp(-.0520 \times 10^{-3} N)$

Mid strain range: $\sigma = 40{,}180 \exp(-.1963 \times 10^{-3} N)$

High strain range: $\sigma = 69{,}900 \exp(-.0556 \times 10^{-3} N)$

The postulated exponential behavior turns out to be not truly exponential; furthermore, as seen from the reduced data, no significant amount of relaxation was observed.

After the cyclic history was completed, the uniaxial specimen was reloaded and observed to exhibit a strain hardening tendency with a higher yield point and further plastic flow paralleling the original flow stress curve. This increase in yield point and continued flow stress curve above the original loading points out that no relaxation (softening) occurred in the uniaxial specimen. If significant relaxation had been present, the yield point would have been lower and failure of the flow stress to match the original curve, due to the recovery that had taken place, would have occurred.

C. DUAL AMPLITUDE CYCLIC LOADING TEST

1. Description of Test

With the data base established for the single amplitude stress recovery behavior, knowledge of the interaction effects of variable amplitude cyclic loading on stress recovery in uniaxial specimens of 7075-T651 aluminum was desired for comparison. This was done using dual amplitude loading to investigate the effects of the lower amplitude on a high-low amplitude cyclic history.

The MTS system's function generator only has single amplitude capability. The use of an analog computer and the beat phenomena was used to generate the dual amplitude cyclic history for the stress relaxation behavior. A function with a low, positive amplitude of one half that of the high amplitude was desired (Fig. 16). Optimum utilization of the system required a high amplitude output voltage of + 10.0 VDC, and a maximum low amplitude output voltage of + 5.0 VDC was selected for the other cycle.

Two basic sinusoidal signals are added to create the dual amplitude signal (Ref. 8 and 9).

$$X_1 (t) = R_1 \text{ Cos } (\omega_1 t)$$

$$X_2 (t) = R_2 \text{ Cos } (\omega_2 t)$$

are combined to give

$$X (t) = R \text{ Cos } (\omega_1 t + \phi).$$

Summing of the two functions, $X_1(t)$ and $X_2(t)$, produced the

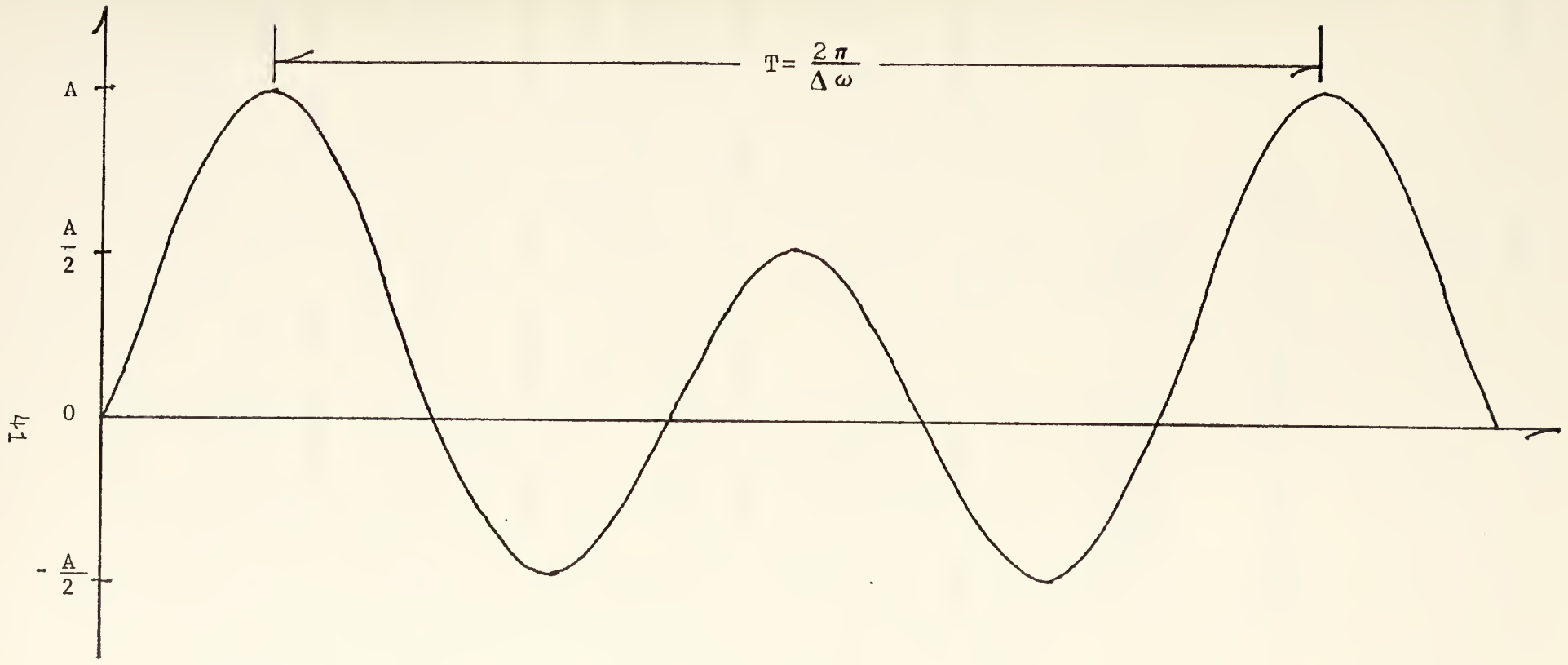

Figure 16
Dual Amplitude Input Function

resultant, X(t), where

$$X(t) = X_1(t) + X_2(t)$$

Also,

$$R = \left[R_1^2 + R_2^2 + 2R_1R_2 \cos(\Delta\omega t)\right]^{\frac{1}{2}}$$

and

$$\tan\phi = \frac{R\sin\phi}{R\cos\phi} = \frac{-R_2 \sin(\Delta\omega t)}{R_1 + R_2 \cos(\Delta\omega t)}$$

where $\Delta\omega = \omega_1 - \omega_2$ and $T = 2\pi/\Delta\omega$ can be written.

Consideration of Figure 16 and the conditions that R=10.0 at the high amplitude output and R=5.0 at the low amplitude output, allowed constraint equations to be written in the form $X(t) + \Delta = R$, where Δ was a constant voltage added to give an additional degree of freedom with which to force the resultant output into a dual amplitude wave form. The constraint equations obtained were $X(0) + \Delta = 10$ and $X(T/2) + \Delta = 5$. An additional constraint equation was obtained from the negative portion of the desired waveform, where $R = -5.0$ was arbitrarily chosen such that $X(T/4) + \Delta = -5.0$. The application of the expressions for $R(t)$, $\phi(t)$ and $X(t)$ to the above constraint equations at t=0, t=T/4 and t=T/2 gave rise to three equations in three unknowns for solution. For these calculations $\omega_1 = 2\Delta\omega$ was desired for only two amplitudes to be produced per cycle. At t=0, $\phi(0)=0$, $R(0)=R_1 + R_2$ and $X(0) = R(0) = R_1 + R_2$ and $R_1 + R_2 + \Delta = 10$.

At $t = T/4$, $\Delta\omega t = \Delta\omega T/4 = \pi/2$, and $\omega_1 t = \pi$,

then,

$$\text{Tan}\,\phi(T/4) = \frac{-R_2}{R_1} \quad , \quad R(T/4) = \left[R_1^2 + R_2^2\right]^{\frac{1}{2}}$$

and

$$X(T/4) = \left[R_1^2 + R_2^2\right]^{\frac{1}{2}} \text{Cos}\left[\pi + \phi(T/4)\right] \quad .$$

By use of a trignometric identity the equation

$$X(T/4) = -\left[R_1^2 + R_2^2\right]^{\frac{1}{2}} \text{Cos}\,\phi(T/4)$$

could be written. Then, if a right triangle is constructed with R_1 and R_2 as sides and $\left[R_1^2 + R_2^2\right]^{\frac{1}{2}}$ as the hypotenuse, $\phi(t)$ is the angle between the hypotenuse and R_1. Therefore,

$$\text{Cos}\,\phi(t) = \frac{R_1}{\left[R_1^2 + R_2^2\right]^{\frac{1}{2}}} \quad ,$$

which, when substituted into the equation for $X(T/4)$, yielded $X(T/4) = -R_1$ . . Then, $-R_1 + \Delta = -5.0$ could be written.

At $t = T/2$, $\Delta\omega t = \Delta\omega T/2 = \pi$, and $\omega_1 t = 2\pi$ then,

$\phi(T/2) = 0$, $R(T/2) = R_1 - R_2$, and $X(T/2) = R_1 - R_2$.

Then, $R_1 - R_2 + \Delta = 5.0$ .. Thus, three equations

$$\begin{aligned} R_1 + R_2 + \Delta &= 10 \\ -R_1 + \quad + \Delta &= -5 \\ R_1 - R_2 + \Delta &= 5 \end{aligned}$$

were available for solution to obtain R_1, R_2, and Δ . Simultaneous solution of the equations gave values of $R_1 = 6.25$, $R_2 = 2.50$ and $\Delta = 1.25$.

Having established the amplitudes required to generate the desired function, the frequences ω_1 and ω_2 were considered next. The requirement to keep the periodic output function rate low to remain within system and recorder limitations led to the selection of $\omega_1 = \pi/5$ rad/s. Having assumed $\omega_1 = 2\Delta\omega$, it follows that $\Delta\omega = \pi/10$ rad/s and $\omega_2 = \pi/10$ rad/s. This established the beat frequency, f, at f = 0.05 Hz and period, P, equal to 20 s/c. Thus, the period for one local oscillation, from high peak amplitude to the next corresponding low peak amplitude, was 10 s/c.

The input functions thus obtained were

$$X_1(t) = 6.5 \text{ Cos}(\pi/5t)$$

and

$$X_2(t) = 2.5 \text{ Cos}(\pi/10t) \quad .$$

To produce these functions, differential equations for analog solution were programed as follows:

$$\ddot{X}_1(t) = -0.3948 \; X_1(t)$$

and

$$\ddot{X}_2(t) = -0.0987 \; X_2(t) \quad .$$

The two input functions were summed with $\Delta = 1.0$ VDC at the final stage, prior to input of the resulting function to the controller of the system, to provide alternating, maximum positive amplitude peak output voltages of +10.0 and + 5.0 VDC .

To prevent compressive yield in the specimen due to the -5.0 VDC output on each cycle of the function, the reference voltage or local zero of the system, was set such that, under strain control, the negative voltage output caused the specimen to be placed in a state of zero strain. Maximum strain was set to 5.1 VDC output of the 10.0 VDC available. This corresponded to 0.0075 in/in strain in the specimen on the high amplitude cycle and 0.0038 in/in strain on the low amplitude cycle.

The test was initialized by first straining the specimen into the plastic range to the same degree as the single amplitude cyclic tests. This was done to compare the dual amplitude effect with the same initial strain as the single amplitude specimens.

After the initial strain was introduced into the specimen, control of the MTS system was transferred to the analog computer. The initial conditions were set to zero at the start of the test and then brought up to the specified values manually with the system under the control of the analog computer. With all initial conditions set in, the specimen was in a maximum strain condition for the high amplitude cycle. At this point the analog computer was activated and allowed to cycle the specimen 150 times. Outputs of strain and load voltages were recorded on both the X-Y recorder and the dual trace strip chart recorder. As in previous tests, the load cyclic voltages were also recorded manually for a more accurate reduction of relaxation behavior.

2. Test Results

Output voltages of stress and strain recorded by the X-Y recorder provided data to produce a monotonic stress-strain curve (Fig. 17 and Table 13). The modulus of elasticity for the initial loading was calculated to E=10.35 x 10^6 lbf/in^2. The first indication of the proportional limit appeared at 53,570 lbf/in^2 and a yield stress at 74,000 lbf/in^2. The measurements agreed with accepted values. The .2% offset yield stress was 2,000lbf/in^2 higher than the 72,000lbf/in^2 listed in metal handbooks.

The dual trace recorder provided a load output voltage record, which was also recorded manually to give a more accurate record of the cyclic load reduction throughout the test. This load voltage provided the data base from which the maximum stress per cycle could be computed (Table 14). The log stress data was plotted versus cycle number, N, on semilog graph paper (Fig. 18) to graphically represent the stress decay behavior occurring in the dual amplitude interaction. The log plot produced a small amplitude sine wave function when expanded, but it was essentially a straight line. Equations for both stress decay behaviors would again appear to be of the form $\sigma = \sigma_o \exp(-bN)$. An exponential curve fit was applied to 75 high stress points and to 75 low stress points out of the 150 cycles used during the test sequence. As in the single amplitude test, a poor correlation factor was evident. The resulting equation for the high amplitude stress recovery behavior was

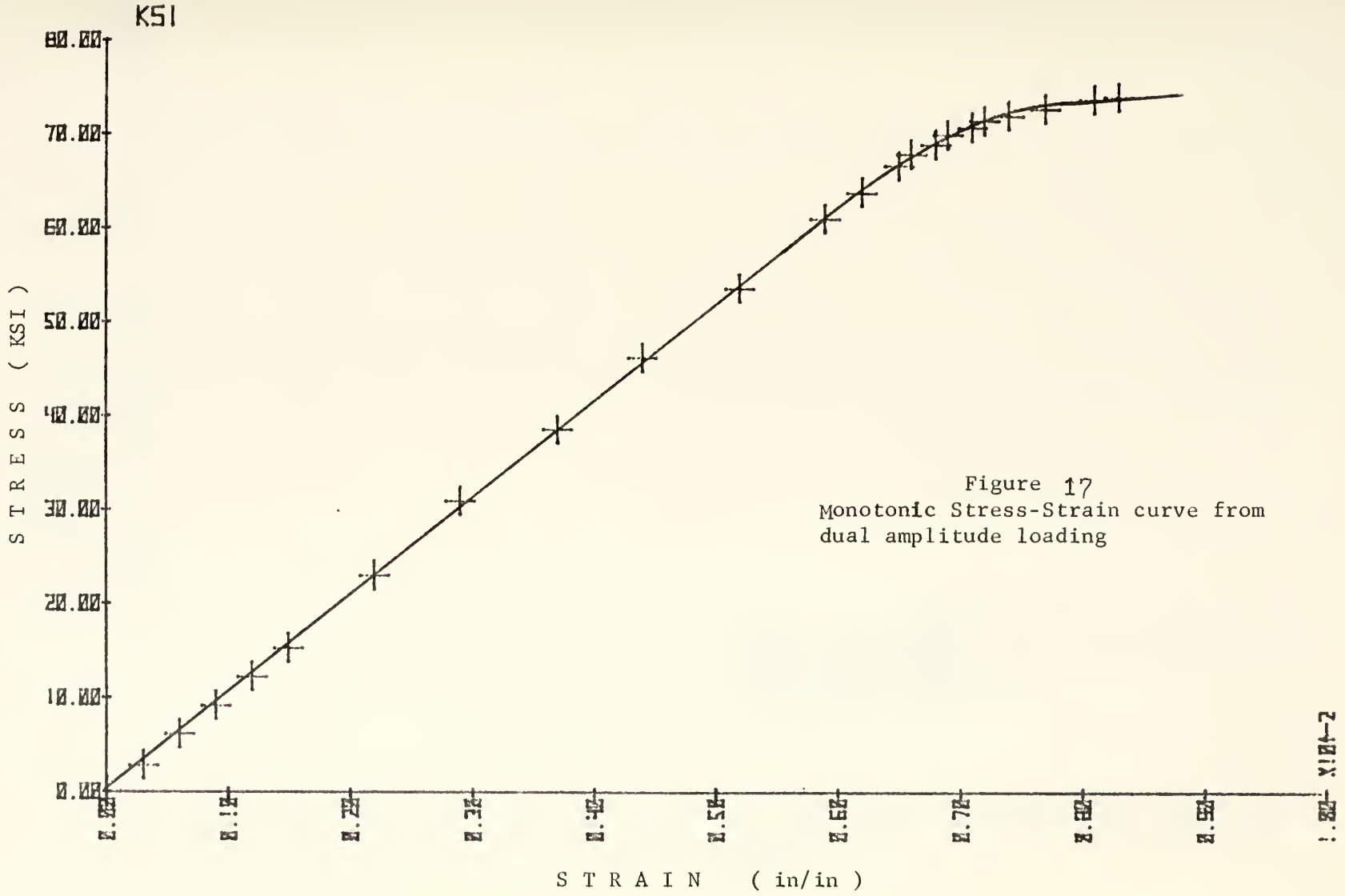

Figure 17
Monotonic Stress-Strain curve from dual amplitude loading

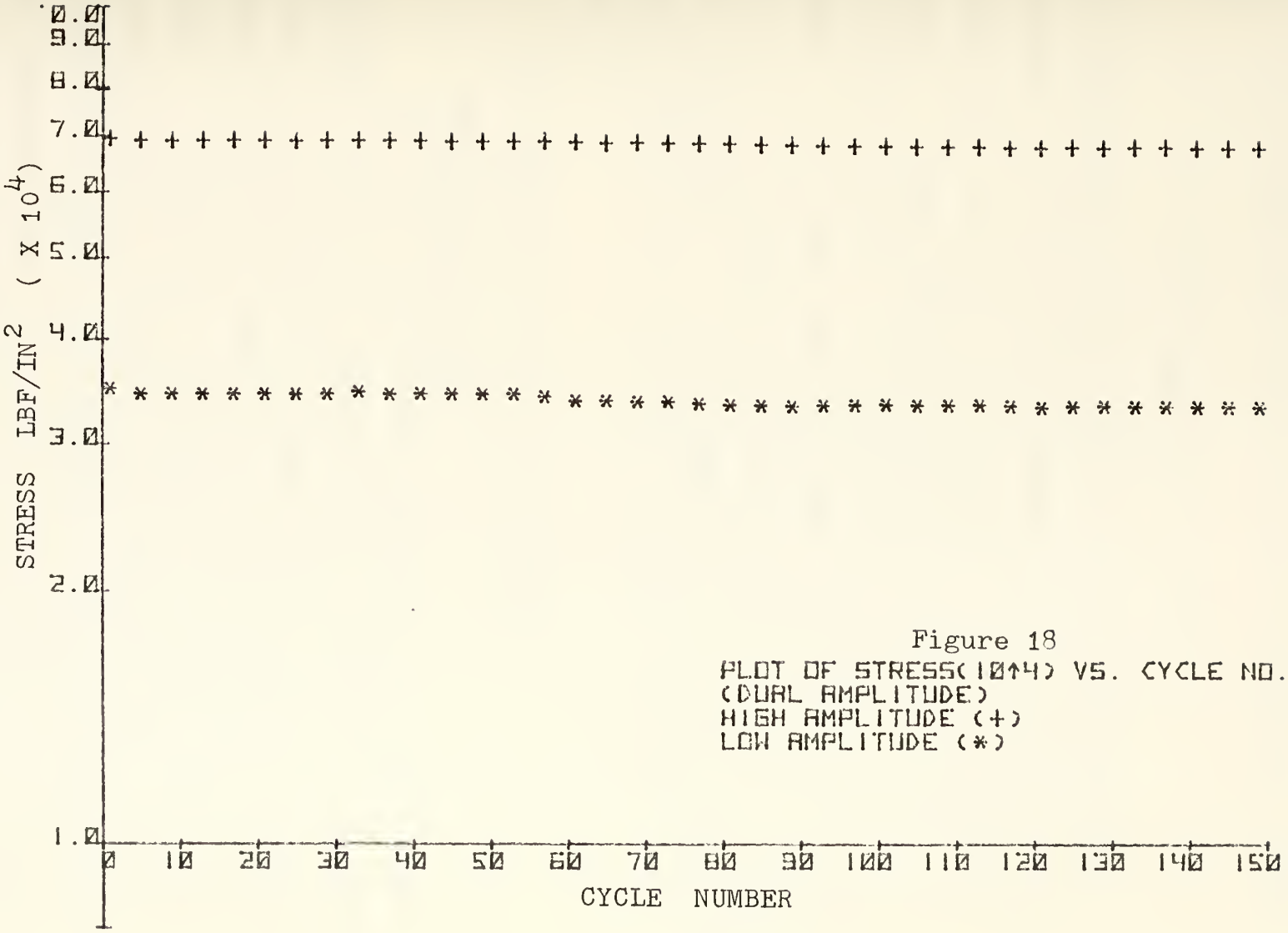

Figure 18
PLOT OF STRESS(10↑4) VS. CYCLE NO.
(DUAL AMPLITUDE)
HIGH AMPLITUDE (+)
LOW AMPLITUDE (*)

$$\sigma = 69{,}600 \exp(-.1693 \times 10^{-3} N) \quad .$$

For the low amplitude stress situation the equation reduced to

$$\sigma = 35{,}000 \exp(-.3312 \times 10^{-3} N) \quad .$$

The stress decay behavior of the high and low amplitudes exhibited a 60.7% and 40.7% increase over the similar strain range single amplitude cyclic history. Thus the stress behavior in a dual amplitude history was shown to exhibit an interaction between the dual amplitude strain levels. As shown in the single amplitude tests, the dual amplitude data had a poor correlation factor when curve fit to the exponential relationship. It was shown not to be a true exponential decay evidenced by b not being a constant as illustrated in (Fig. 19).

D. CYCLIC BEHAVIOR OF 7075-T651 ALUMINUM

1. Description of Test

The test conducted was controlled by a fixed strain amplitude, wherein the specimens were loaded into the plastic range by a predetermined voltage setting being varied plus or minus by a sine wave produced by the function generator internal to the MTS unit. The use of the Hewlett-Packard X-Y recorder enabled a record of the hysteresis action during the test sequence to be maintained. The cycle frequency for the hysteresis test was 0.05 Hz. Two identical tests were conducted to substantiate the information comparing the two loops to offset any material faults in the uniaxial specimens.

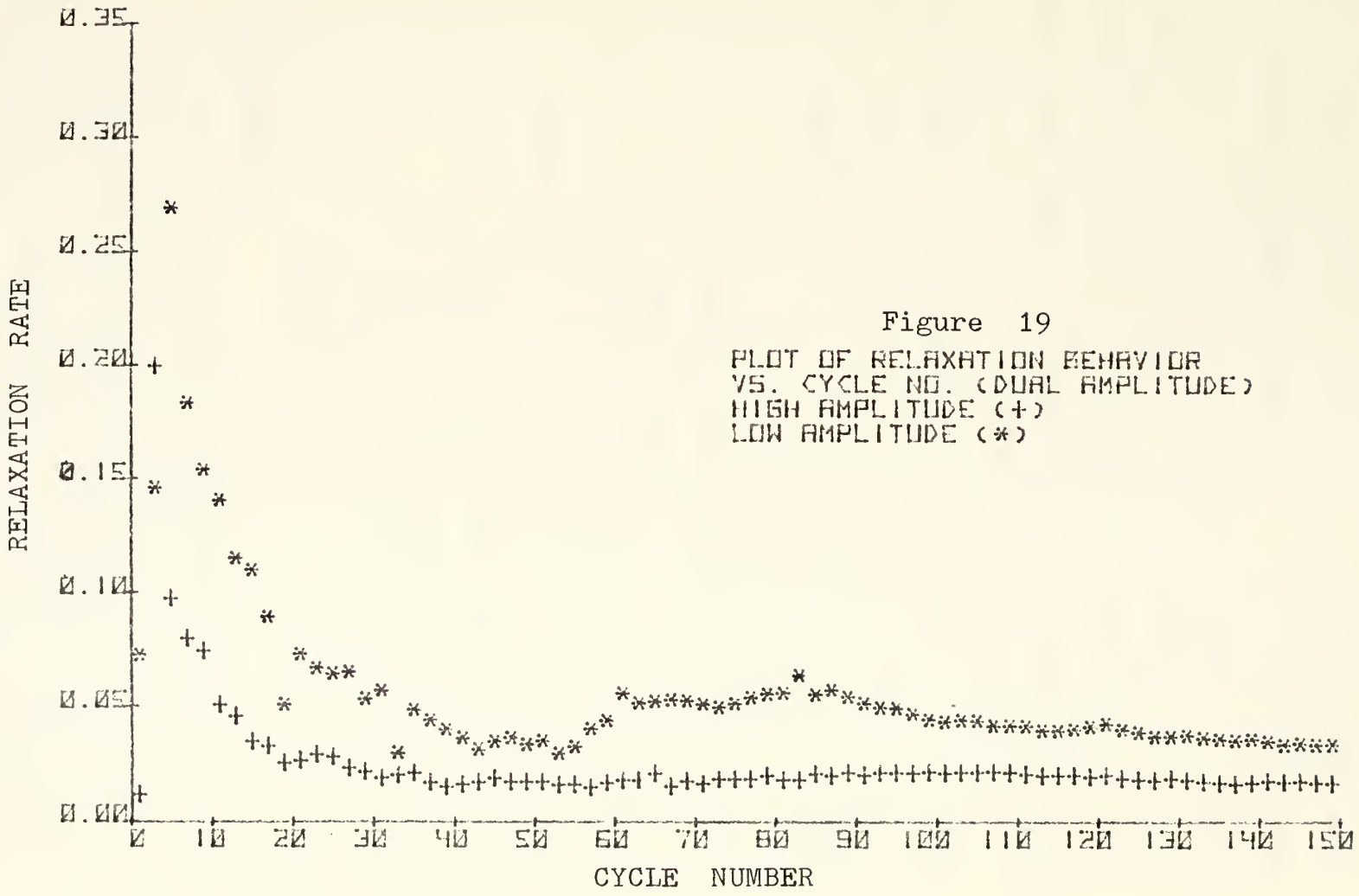

Figure 19

PLOT OF RELAXATION BEHAVIOR
VS. CYCLE NO. (DUAL AMPLITUDE)
HIGH AMPLITUDE (+)
LOW AMPLITUDE (*)

To investigate the cyclic behavior further, a series of tests were conducted utilizing the same uniaxial specimen for all the repeated loadings. The cycling was done from zero strain to maximum strain, 0.009 in/in. The strain history was controlled by the function generator internal to the MTS system under a haversine function at 0.05 Hz similar to the full hysteresis loop test. The load was monitored on the X-Y recorder and recorded manually at each maximum excursion of the haversine function. After 150 cycles, the specimen was unloaded and the extensometer was detached. The cycled specimen was then treated as a new unloaded specimen for each of the remaining five loading and three cyclic periods. This segment of tests was conducted to investigate the possible interaction of relaxation and strain hardening in load histories on the same tensile specimen. To substantiate the effect of strain hardening of the specimen after repeated loadings, a hardness test was performed on an unloaded specimen, after the first cyclic loading, and after the fifth loading history. This type of test sequence was done in an effort to simulate the flight spectrum load histories subjected to the aircraft structure.

2. Test Results

The X-Y recorder plot of output voltages of load and strain provided a series of hysteresis loops, each being cycled to the same fixed strain. The initial loading of the specimen provided an opportunity to construct a monotonic stress-strain curve (Fig. 20 and Table 2) from the observed load and strain recordings The .2% offset yield stress

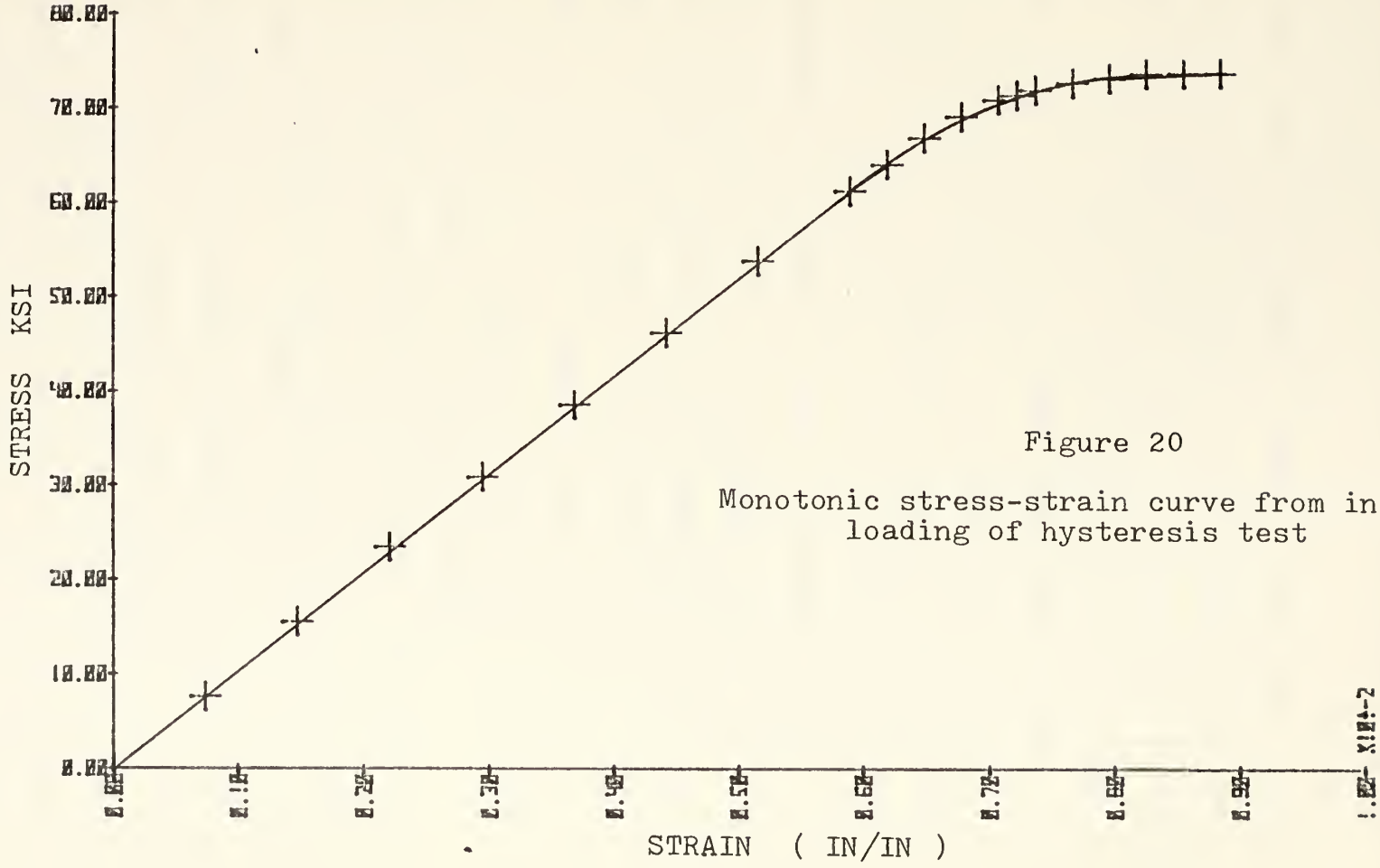

Figure 20

Monotonic stress-strain curve from initial loading of hysteresis test

obtained from the initial loading segment was found to be 73,580 lbf/in^2. This yield stress and the calculated modulus of elasticity, 10.48 X 10^6 lbf/in^2, correspond favorably with the accepted values.

In the cyclic hysteresis loading, relaxation was not observed by the slight stress level increase required to attain the controlled strain level. In the case of 7075-T651 aluminum, cyclic strain hardening(increase in stress range) was found to occur at the strain amplitude selected. The shift in the upper tips was relatively small compared to that of the lower tips. An apparent change in the hysteresis loop shape with the occurrence of each cycle was noted. When various branches are compared along the elastic slope, it is seen that the yield point is changing slightly with cycle, while the actual branches of the hysteresis loop are almost the same in overall shape. While relaxation is denoted by a decrease in yield point between cycles, the increase in its value with cycles, as observed in the test conducted, denotes hardening when compared to similar reversals.

In the single specimen load history, tests have indicated a definite tendency of the metal to strain harden during the cyclic load history. A Rockwell hardness test was taken before loading the specimen and after the second and fifth loading to further demonstrate the hardening of the lattice structure. The values taken on the Rockwell B scale were 89.0, 89.4 and 89.8, respectively. Thus, the Rockwell results showed a slight hardening behavior. The change in the yield point between the initial and fifth loading sequence

is illustrated in (Fig. 21) and (Table 3 and 4). The observed character of the material after repeated loadings, approached an elastic perfectly plastic type of behavior.

There was marked increase in stress decay while cycling continuously into the plastic range of the material rather than in the elastic range after as initial plastic loading. The relaxation rate behavior as function of initial applied stress and cycle number for the test sequences are illustrated in (Figs. 22, 23 and 24). It was noted that during the decay process to stabilization the b exponent in the exponential relationship, $\sigma = \sigma_o \exp(-bN)$, was not a constant. From a plot of the log stress versus cycle number, a slope was found to indicate that the value did appear to act in an exponential manner, but again the b exponent was not a constant. The slope of the plot gave an indication of the overall stabilization rate behavior. The expressions were found to be as follows:

$$\sigma = 73{,}720 \exp(-.1966 \times 10^{-3} N)$$

during the initial loading and cyclic sequence,

$$\sigma = 75{,}510 \exp(-.1518 \times 10^{-3} N)$$

after the second loading and cyclic sequence,

$$\sigma = 77{,}200 \exp(-.1471 \times 10^{-3} N)$$

after the fourth loading and cyclic sequence.

The diminishing values show that a smaller amount of stress decay occurred ater each consecutive loading history.

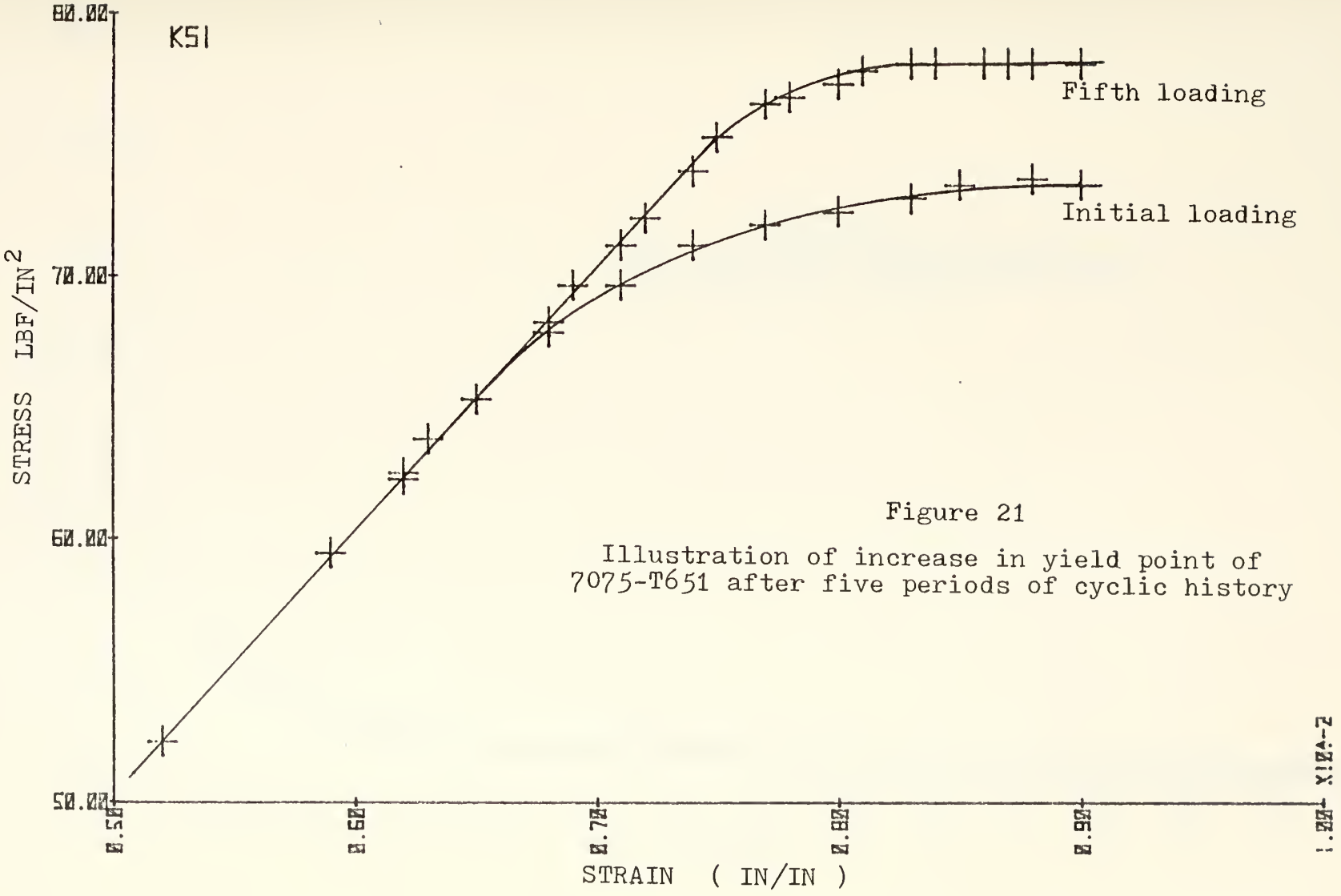

Figure 21

Illustration of increase in yield point of 7075-T651 after five periods of cyclic history

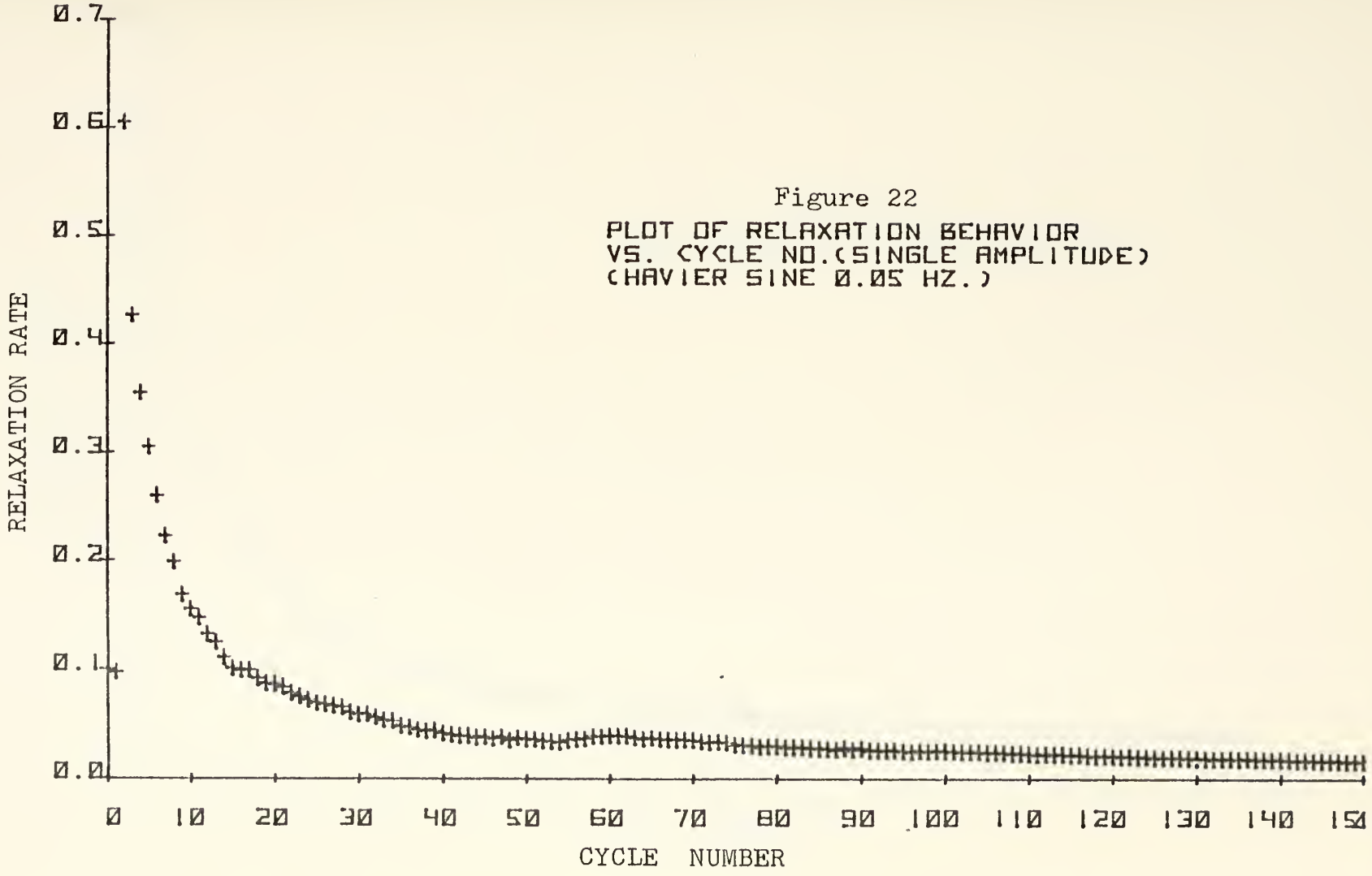

Figure 22
PLOT OF RELAXATION BEHAVIOR
VS. CYCLE NO.(SINGLE AMPLITUDE)
(HAVIER SINE 0.05 HZ.)

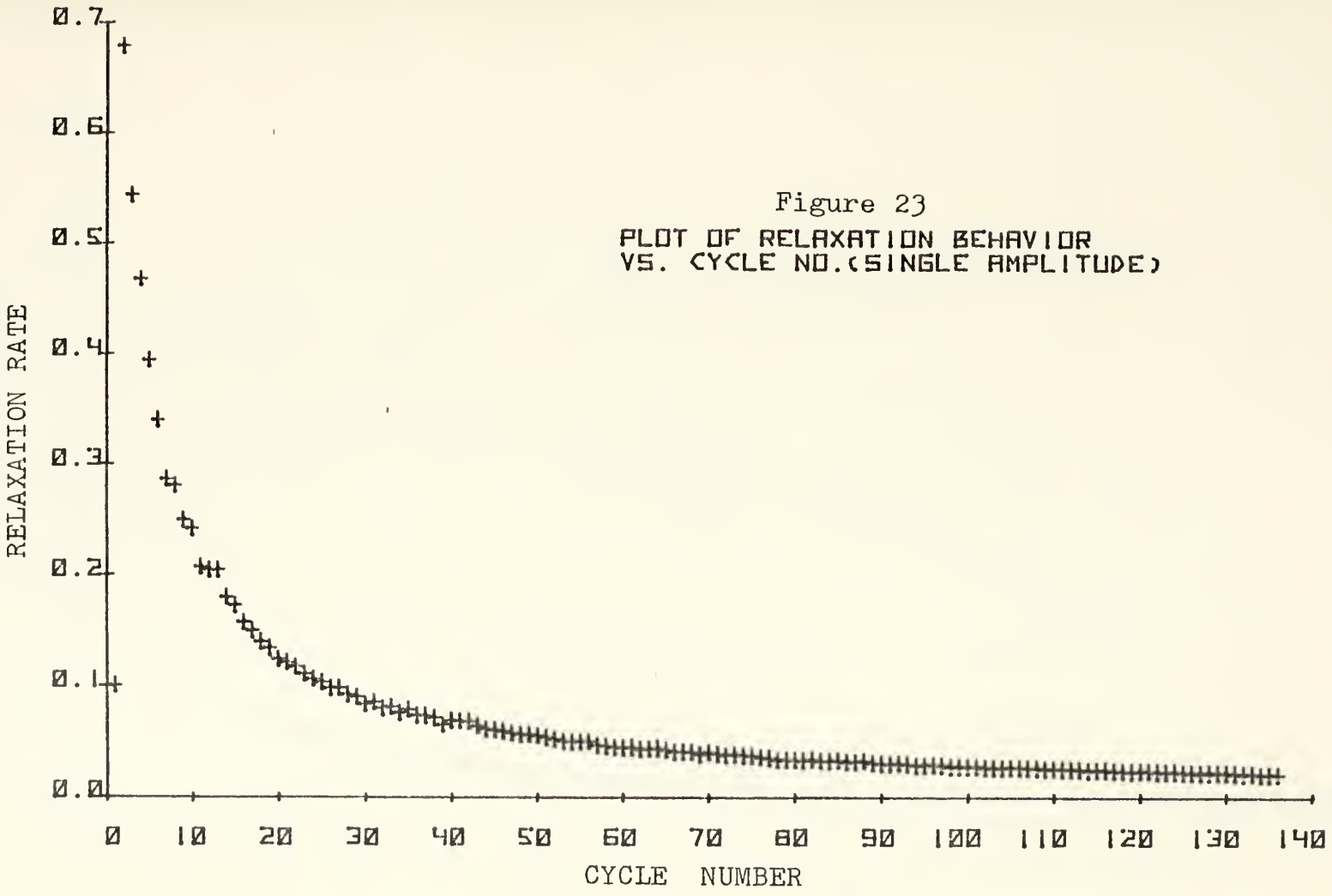

Figure 23
PLOT OF RELAXATION BEHAVIOR
VS. CYCLE NO.(SINGLE AMPLITUDE)

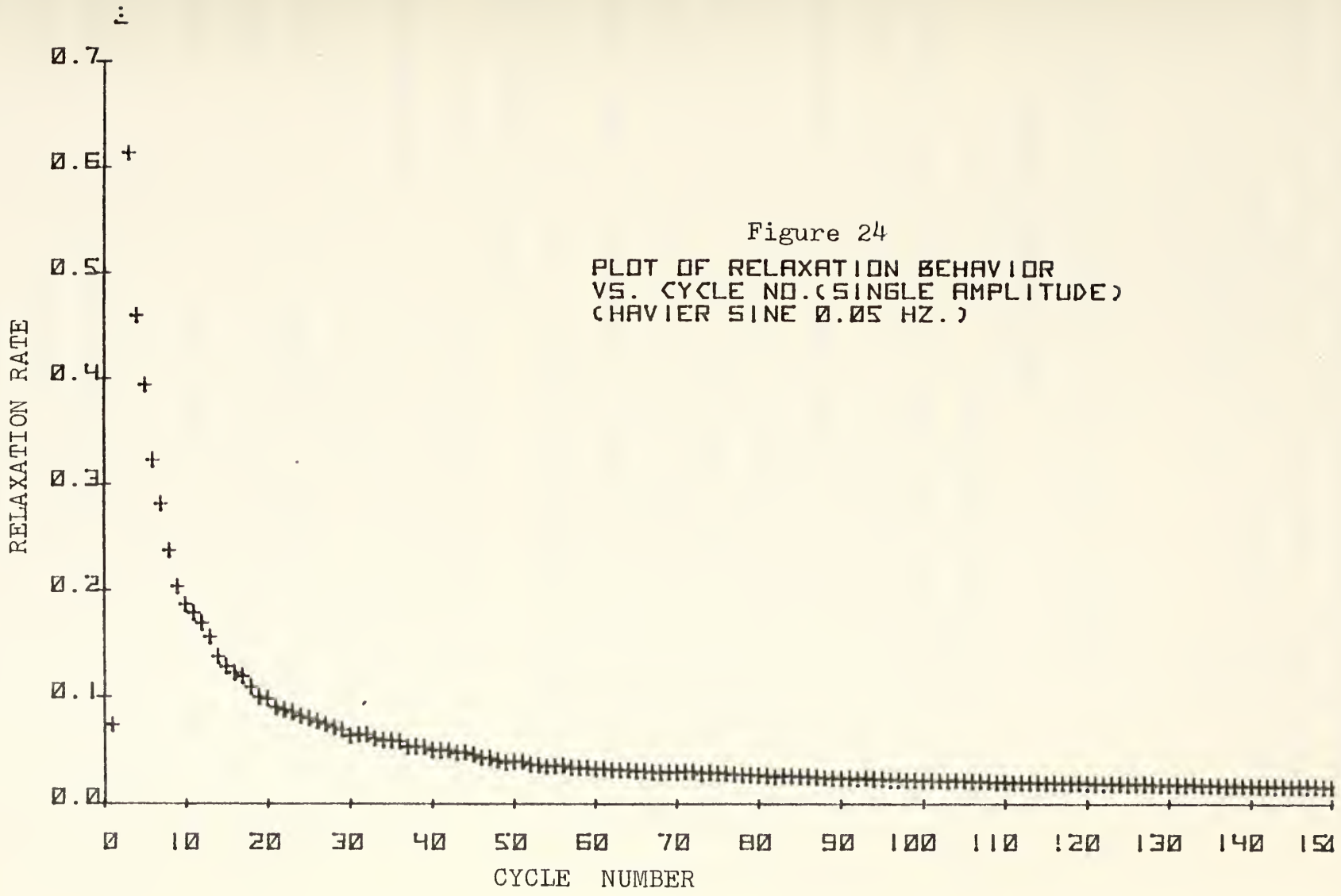

Figure 24

PLOT OF RELAXATION BEHAVIOR
VS. CYCLE NO.(SINGLE AMPLITUDE)
(HAVIER SINE 0.05 HZ.)

As viewed from the figures illustrating the relaxation behavior as a function of cycle number it was evident that time to stabilization was increasing with each cyclic history. The tabular data can be seen in (Tables 5, 6, and 7).

E. ANELASTIC BEHAVIOR OF 7075-T651 ALUMINUM

1. Description of Test

To investigate the anelastic behavior of 7075-T651, a uniaxial specimen was loaded into the plastic range at 0.0005 in/sec strain rate, and unloaded to zero load under load control corresponding to 0.005 in/in strain. Upon reaching zero load, the strain was monitored for one and a half hours. Two tests were done at similar strain amplitudes to substantiate any material defects present. Strain data was monitored by the use of the MTS extensometer and the strain voltage was manually recorded from the digital voltmeter.

To determine if this anelastic action is strictly time dependent or if it is influenced by cyclic loading, two separate tests were conducted. The two tests were similar to the first anelastic sequence in that they were loaded to the same level of plastic strain and then unloaded under load control to zero load. The first of these two tests was allowed to set at zero load for one hour and then cycled for fifty cycles between zero load and 25,500 lbf/in^2 at 0.05 Hz under a haversine wave form. The recovery strain was monitored as a function of time. The next test was

reversed, cycling first and then allowing the sample to set at zero load for one hour.

2. Test Results

After the elapsed time, a decrease was observed in the accumulated plastic strain. The strain transient associated with anelastic strain and/or structural recovery is clearly seen in (Figs. 25 and 26) and (Tables 8 and 9). The two figures illustrate the type of strain recovery which the metal exhibited. In the two tests a 7.02% and a 5.17% recovery of plastic strain occurred. This amount of anelastic recovery is an appreciable amount relating to a stress level decay of 3,900 lbf/in^2 and 2,688 lbf/in^2, respectively. To substantiate the effect of anelastic recovery accounting for the observed plastic strain recovery and not a "relaxation" behavior occurring, the specimens were reloaded toward failure. As seen in (Fig. 3), the flow curve paralleled the unloading with a small amount of knee joining into the expected continuation of the flow curve. If any "relaxation" recovery had been experienced by the lattice structure, there would have been a softening and a failure of the material upon reloading to obtain the original flow curve as illustrated by the lower dashed line in (Fig. 3). It is conclusive that an observed anelastic behavior is experienced in 7075-T651 aluminum alloy.

In the second phase of testing it was found that the cycling of the specimen does not contribute significantly to the recovery of plastic strain. In both test sequences

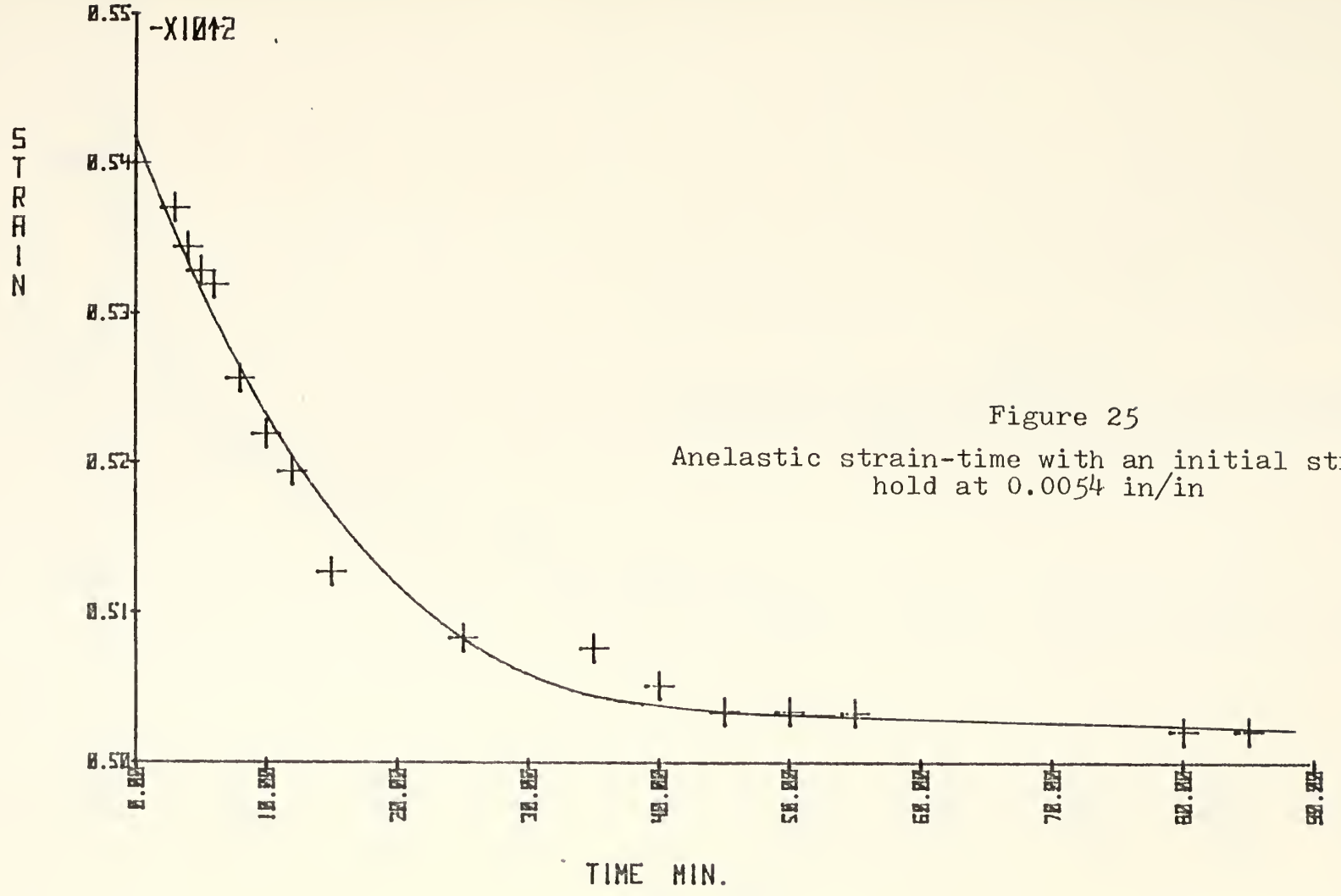

Figure 25

Anelastic strain-time with an initial strain hold at 0.0054 in/in

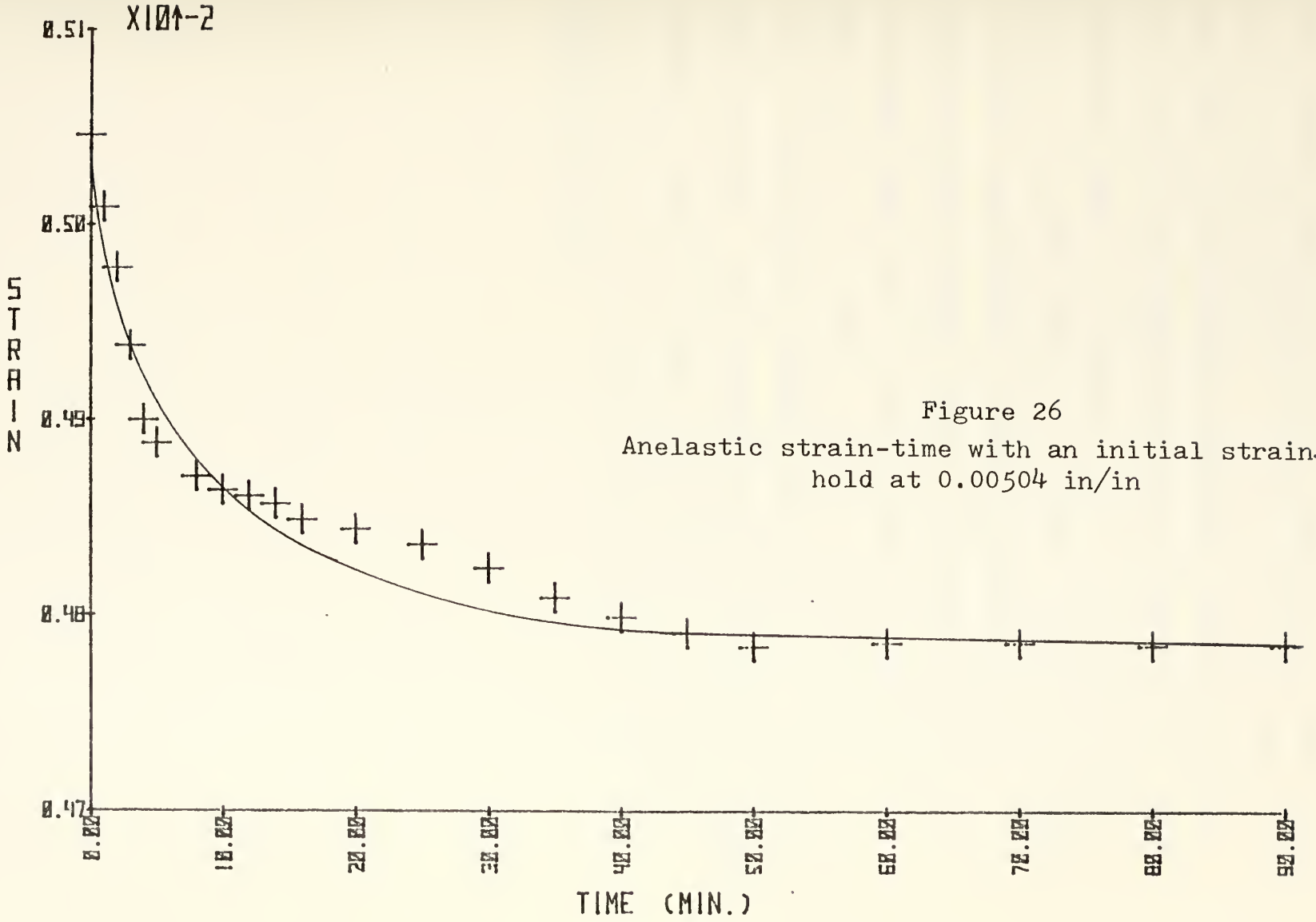

Figure 26
Anelastic strain-time with an initial strain hold at 0.00504 in/in

the same amount of plastic strain was recovered. The tests utilized previously cycled material to check on previous history effects. In the first test it was noted that all the plastic strain was recovered in the static period preceeding the cyclic loading, which contributed no strain recovery. In the second test the cyclic loading was carried out first. Half of the plastic strain was recovered during this phase and the remaining plastic strain during the static portion. It is evident that once the substructural recovery has taken place in the static portion, the subsequent cyclic history has an insignificant effect on the plastic strain recovery. Upon reloading the specimens to approach failure, a slight increase was noted in the yield point indicating the cyclic segment did contribute a strain hardening behavior.

IV. DISCUSSION OF TEST RESULTS

During the cyclic history sequence three stress-strain curves were constructed from the data recorded on the X-Y recorder. The curves were constructed for the initial cycle of the hysteresis curve, the initial loading of the single specimen multi-loading sequence, and the dual amplitude loading history. These stress-strain curves provided a means of comparing the consistency between the test specimens.

The three moduli of elasticity from these separate tests were 10.48×10^6 lbf/in^2, 10.08×10^6 lbf/in^2, and 10.35×10^6 lbf/in^2 respectively. The average value of the three moduli of elasticity proved to be 10.31×10^6 lbf/in^2, which agrees with the established modulus of 10.30×10^6 lbf/in^2 for 7075-T651 aluminum. Comparison of curve shape indicates excellent linearity up to 63,300 lbf/in^2, after which the strain hardening varied in the three uniaxial specimens.

In the hysteresis tests, the strain hardening behavior of 7075-T651 was investigated. A slight increase in the stress range at the upper strain limit was observed. An increase in the stress range at the lower limit with an increasing yield point denoted strain hardening behavior. Substantiation of the strain hardening behavior was obtained via the sequence of tests utilizing the same uniaxial specimen

under multi-loading histories. The tests consisted of five loadings and three cyclic loading periods. After each loading to the maximum strain limit there was a pronounced increase in the yield point. Maximum increase occurred in the first three loadings. After the fifth loading there was little increase in yield point. Since the stress required to produce a fixed strain increased in successive cyclic loadings, and since the Rockwell hardness tests indicated a coincident hardening, this material, after successive loadings, approaches an elastic perfectly plastic material as utilized by Potter in his relaxation model Ref. 2.

The phenomenon of transient hardening or softening associated with relaxation is an inherent material feature that prevents a study of pure relaxation behavior. It always occurs during step changes in strain or stress amplitude irrespective of whether the material has been previously stabilized by cyclic loading or not. Present formulations to simulate cyclic stress-strain response ignore this feature and assume that step changes in strain amplitude are accompanied by corresponding step changes in stress amplitude responses by the material. Consequently, these models continuously harden or soften to stablization at a rate defined by a cumulative parameter such as the cumulative plastic strain or number of cycles and cease to harden or soften once stabilization has occurred.

The relaxation behavior as utilized in the relaxation models indicated a decrease in relaxation rate after each successive cycle. An increase in the transient stress decay

rate by 43% was observed whencycled continually into the plastic range instead of cycling only in the elastic region. From these observations it can be concluded that the material strained constantly into the plastic range, as would be found at stress concentrations, would have a higher stress decay rate to stabilization. The time to stabilization for the elastic cyclic history was found to be 10% longer, demonstrating the difference in stabilization rate.

The higher the initial stress amplitude, the faster the material stabilized at a steady stress level. Saturation was found to occur within 20% of the cycle lif used.

The interaction of the dual amplitude test sequence denoted an increase in the extent of stress decay in the low amplitude loadingover the high amplitude by 18%. The dual amplitude also demonstrated the difference in time to stabilization. The high amplitude gaining equilibrium by 13.3%, and the low amplitude by 33.3% of the cyclic test life. When comparing the single and dual cyclic histories, an increase in the stress decay behavior of both high and low amplitudes when compared to the decay rate behavior of the single amplitude histories was observed. A possible sensitivity to multi-load history was indicated.

The investigation into recovery mechanisms included an anelastic test sequence. There was a definite anelastic behavior as denoted in Figure 26 and 27. Due to the strict definition of relaxation, it is noted that the stress recovery process is not strictly a relaxation process illustrated by the fact that upon reloading the uniaxial specimen it did in fact rejoin the stress flow curve. If

there would have been a recovery process taking place as relaxation, a softening of the lattice would have occurred and the material would failed to rejoin the original flow curve. Instead, it would have continued below the original curve and would have had a lower yield stress. It is felt that the substructural recovery process is an anelastic time dependent process, rather than a relaxation behavior driving the material to substructural stabilization during load time history.

V. CONCLUSIONS AND RECOMMENDATIONS

The major point of intent in this thesis has been to establish a relevant mode of plastic strain recovery to account for the dimenishing value of stress during the structural material life cycle. It was pointed out that a possible misnomer of the recovery mechanism in 7075-T651, accounting for this behavior, had been made.

The first area of interest was in the substructural recovery, by relaxation of the lattice structure, that acounts for the stress decay toward a stabilized stress level. From the cyclic test results it can be concluded that true relaxation is not the prime or even the secondary mode of the recovery process. To restate that relaxation is not occurring is evident in the reloading of the uniaxial specimens after the various load histories have shown no softening (recovery) taking place. Consistently in every test the flow stress curve was rejoined at the original flow curve and after cyclic loading showed a strain hardening behavior.

The diminishing stress level when treated by the relationship, $\sigma = \sigma_o \exp(-bN)$ did follow an approximate exponential decay in stress as a function of initial loading and cycle number. The rate of stress decay to stabilization was shown to increase significantly if the cyclic history included cycling into the plastic region and also included a compressive period. The compressive period may have acted as an accelerating factor due to the Baushinger effect. By

experiencing a slight compressive loading this acted to reduce dislocation back stress that had been built up during this reloading phase in the tensile loading. Therefore, on reloading the uniaxial specimen it would require less applied stress to reach the strain limit called for in the test history. The material, through its strain hardening behavior was still able to be reloaded to the original stress, discounting any recovery(softening) having occurred to account for the stress decay. Once the lattice structure established a dislocation stress equilibrium, the specimen material stabilized at a reduced stress level and was observed to maintain this level throughout the rest of the material cyclic life in the test sequence.

It is concluded that the prime substructural recovery mechanism in this test material was observed to due to an anelastic behavior. As demonstrated in Potter's relaxation model, this same relative approach may be used. Instead of function of cycle number, it is felt that time is a controlling function. This reasoning is backed up by the fact that the two tests run to determine cyclic effect on the anelastic recovery was shown to be a non-determining factor on the amount of plastic strain that was recovered. Therefore, it is felt that time into the loading history may be a determining factor on establishing a stress level that can be used in the structural analysis. The cyclic stress-strain relations are substantially different from the virgin tensile data in the test material. It is imperative that formulation be achieved to base the fatigue analysis on realistic material

properties that have experienced representative load histories.

The uniaxial anelastic behavior of the 7075-T651 test specimens can be correlated to account for this stress decay behavior. As shown in the following illustration, the plastic strain imparted to the material is time dependent on the amount of strain that is recoverable.

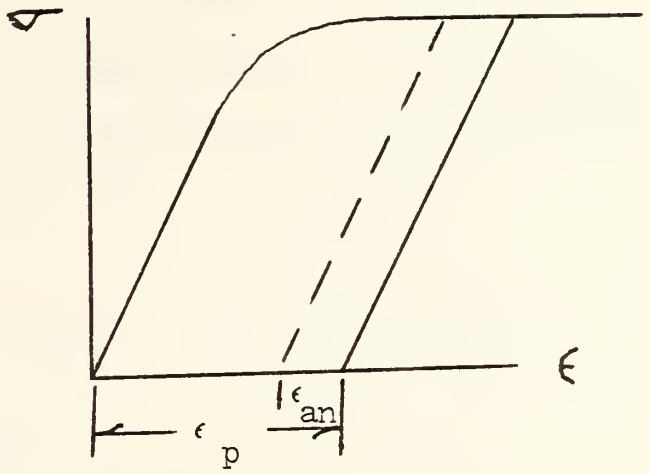

The amount of plastic strain, ϵ_p, is related by $\epsilon_p = \frac{l_p}{l_o}$ as illustrated in the next figure.

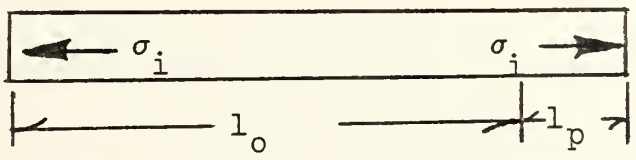

The recoverable plastic strain related to the decay in internal stress required to maintain that strain would be $\sigma_{io} = E\epsilon_p$. Therefore, the remaining internal stress, σ_i, would be

$$\sigma_i = E\,(\epsilon_p - \epsilon_{an})$$

ϵ_{an} being the anelastic recoverable strain. The total strain

imparted to the specimen is $\epsilon = \epsilon_{eq} + \epsilon_{trans}$. To express the total recoverable anelastic strain, ϵ_{trans}, as a function of time, the exponential relation that used cycle number as a controlling factor was used

$$\epsilon_{trans} = A \exp(-bt) \ .$$

Therefore, at time zero, t=0

$$\epsilon_{trans} = \epsilon_p - \epsilon_{eq} \ .$$

The anelastic strain equals the total plastic strain, ϵ_p, minus the equilibrium strain, ϵ_{eq}. By placing the condition t=0, $\epsilon_p - \epsilon_{eq} = A$.
Therefore,

$$\epsilon_{trans} = (\epsilon_p - \epsilon_{eq}) \exp(-bt) \ .$$

then at $t=t_{eq}$,

$$\epsilon_{trans} = 0.1(\epsilon_p - \epsilon_{eq}) \ .$$

It is felt that by experimentation the time taken to achieve 90% of the recoverable strain could be used as a time to reach the equilibrium condition, t_{eq}. By equating the two expressions of ϵ_{trans}, the decay rate may be found,

$$0.1 \ (\epsilon_p - \epsilon_{eq}) = (\epsilon_p - \epsilon_{eq}) \exp(-bt_{eq})$$

reducing to $0.1 = \exp(-bt)$. Therefore,

$$\ln 0.1 = -bt_{eq}$$

$$-b = \ln 0.1/t_{eq} \ .$$

Therefore,

$$\epsilon_{trans} = (\epsilon_p - \epsilon_{eq}) \exp\left[\ln 0.1(t/t_{eq})\right]$$

relating to an internal stress after anelastic recovery equivalent to

$$\sigma_{i(trans)} = E(\epsilon_p - \epsilon_{eq}) \exp(-2.303t/t_{eq}) .$$

This demonstrates the idea of stress recovery due to the anelastic behavior of the material in a tensile loaded uniaxial environment.

The influence exerted by the surrounding elastic material at a stress concentration is postulated in the following illustration.

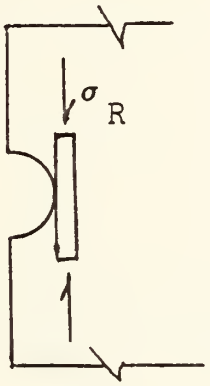

As the anelastic strain, ϵ_{an}, diminishes with time after the initial loading period, the specimen or plastic zone becomes smaller and produces less stress on the surrounding elastic region and, therefore, the residual tress, σ_R, diminishes as a function of time after the peak plastic load was imparted to the stress concentration area. The total residual stress may be thought of as $\sigma_R = \sigma_{Req} + \sigma_{trans}$, therefore,

$$\sigma_R = \sigma_{Req} + (\sigma_{Ro} - \sigma_{Req}) \exp(-2.303t/t_{eq}) .$$

This idea is illustrated in the following figure. It is believed that the residual stress can be expressed in terms

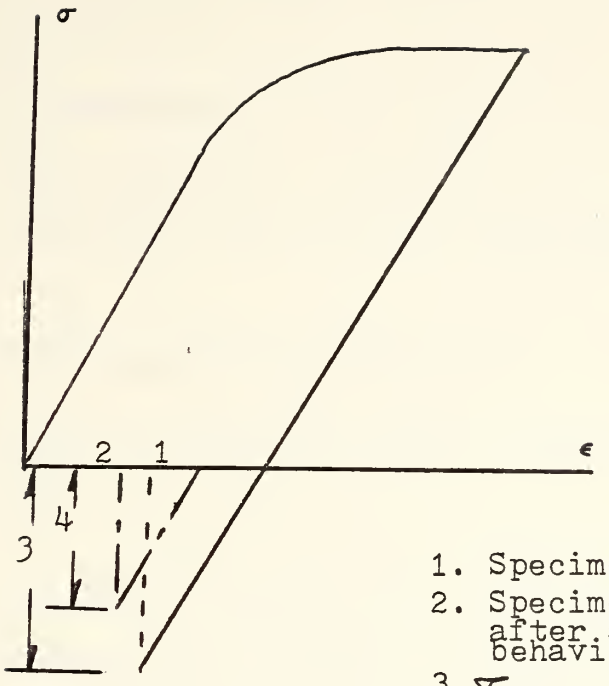

1. Specimen equilibrium
2. Specimen equilibrium after anelastic behavior
3. σ_{Ro}
4. σ_{Req}

of percentage strain recoverable due to the anelastic recovery and time, where $\sigma_{Req} = \% \sigma_{Ro}$ and the $\% = \epsilon_{eq}/\epsilon_p$. Therefore,

$$\sigma_R = \%\sigma_{Ro} + \sigma_{Ro}(1-\%) \exp(-2.303t/t_{eq}) \quad .$$

Factoring out the residual stress at the original plastic strain value simplifies the equation to

$$\sigma_R = \sigma_{Ro} \% + (1-\%) \exp(-2.303t/t_{eq})$$

The residual stress formulation developed here parallels Potter's treatment of relaxation in his model. To compare the test data from the single and dual cyclic amplitude tests to the anelastic behavior, the data from the tests were curve fit using the exponential relation $\sigma = \sigma_o \exp(-bN)$ and in terms of strain $\epsilon = \epsilon_o \exp(-bt)$. The curve fit for the anelastic

behavior proved to show a better correlation factor than the stress decay exhibited by the single and dual amplitude tests. The anelastic factors were 0.74 and 0.61 for the two strain amplitudes, respectively. An anelastic type of decay closer to an exponential behavior was indicated.

The anelastic behavior was reduced to

$$\epsilon = 5.295 \times 10^{-3} \exp(-0.852 \times 10^{-3} t)$$

and

$$\epsilon = 4.919 \times 10^{-3} \exp(-0.444 \times 10^{-3} t).$$

When the two processes are compared, the strain recovery experienced in the anelastic case had a more rapid decay than that of the stress decay in the cyclic stress decay rate test sequence. Both behaviors, however, exhibited an approximate exponential form of decay to stabilization.

Though the two strain levels experienced in the anelastic tests differ by only 6.6%, a 50% difference in decay was observed. It was found with the data available that the times to equilibrium were within 6.4% of each other. The times were 53.49 minutes and 50.05 minutes, respectively. Using MILSPEC A load spectrum of 42,000 cycles experienced in 1000 flight hours, a frequency of 0.7 cycles per minute was calculated. With this load frequency, the cycles to equilibrium under this anelastic behavior was shown to be 35 cycles.

The 35 cycles coincide with the cycles to stabilization experienced during the single and dual amplitude loading

histories. This again substantiates that the process responsible for the stress decay to stabilization is an anelastic recovery process. This time was the point where 90% of the recoverable strain was recovered. This value is arbitrary, but it is felt that by this 90% point the major part of the decay has taken place in the material.

Therefore, with these values put into the equation for residual stress as possible known quantities, the equation simplifies to

$$\sigma_R = \sigma_{R_o} \; 0.9376 + 0.0624 \exp(-0.0919\, t) \quad .$$

By this relationship, the residual stress decay is described in terms of stress at equilibrium, stress at time zero (initial strain level), and time.

Further investigation and evaluation of the effects of ϵ_p on the percentage defined by $\% = \epsilon_{eq}/\epsilon_p$ is needed. More tests using varying levels of strain, ϵ_p, should be conducted. This could establish a definite relationship on how the stress decay may be a function of the initial load strain. Further investigation of this relationship would establish if the time to equilibrium is insensitive to initial plastic loading, as indicated by the limited data shown in this report.

The frequency of events and the degree of unloading after each peak stress is an area of further interest. The degree of unloading is suspected to have an effect on the time to stabilization and the percentage of strain recovered due to the anelastic behavior.

APPENDIX A - TABULAR DATA

TABLE 1

Extensometer calibration data on MTS Model 632.13

Point no.	Extensometer input (mv)	Strain Transducer output (volts)
1	0.0000	0.0000
2	0.1470	0.4530
3	0.2490	0.9790
4	0.5000	2.2490
5	0.7500	3.5450
6	1.0000	4.8640
7	1.2500	6.1180
8	1.5000	7.3670
9	1.7500	8.6410
10	2.0000	9.9310
11	2.2500	11.2350
12	2.5000	12.4800
13	2.6000	13.0500
14	2.7000	13.5400

COEFFICIENTS
B(0)= -0.2291
B(1)= 5.0875
R SQUARE = 0.99976
CORR. COEFF. = 0.99988

STRAIN CONVERSION FORMULA

$$\frac{\text{STRAIN VOLTS}}{5.0875} \times .0075 = \text{STRAIN}$$

Measured in units in/in

TABLE 2

Monotonic stress and strain data from initial loading of hysteresis loop test on a uniaxial specimen.

Load volts	Strain volts	Stress lbf/in^2	Strain in/in
0	0	0	0
.3	.5	7653	0.0007
.61	1.0	15561	0.0015
.92	1.5	23469	0.0022
1.21	2.0	30867	0.0029
1.51	2.5	38520	0.0037
1.81	3.0	46173	0.0044
2.11	3.5	53826	0.0052
2.40	4.0	61224	0.0059
2.51	4.2	64030	0.0062
2.62	4.4	66836	0.0065
2.71	4.6	69132	0.0068
2.78	4.8	70918	0.0071
2.80	4.9	71428	0.0072
2.82	5.0	71938	0.0074
2.85	5.2	72704	0.0077
2.87	5.4	73214	0.0080
2.89	5.6	73724	0.0083
2.891	5.8	73750	0.0085
2.891	6.0	73750	0.0088

TABLE 3

Monotonic stress and strain data on initial loading of a uniaxial specimen under consecutive loadings.

Load volts	Strain volts	Stress lbf/in^2	Strain in/in
0.000	0.0	0	0.0000
0.295	0.5	7525	0.0007
0.600	1.0	15306	0.0015
0.899	1.5	22934	0.0022
1.190	2.0	30357	0.0029
1.480	2.5	37755	0.0037
1.770	3.0	45153	0.0044
2.050	3.5	52295	0.0052
2.330	4.0	59439	0.0059
2.440	4.2	62244	0.0062
2.560	4.4	65306	0.0065
2.660	4.6	67857	0.0068
2.730	4.8	69642	0.0071
2.790	5.0	71173	0.0074
2.820	5.2	71938	0.0077
2.840	5.4	72449	0.0080
2.860	5.6	72959	0.0083
2.880	5.8	73470	0.0085
2.889	6.0	73698	0.0088
2.889	6.1	73469	0.0090

TABLE 4

Monotonic stress and strain data on the fifth loading after cyclic history complete on the same uniaxial specimen.(data beginning at 4.2 volts in linear portion of stress-strain curve)

Load volts	Strain volts	Stress $_2$ lbf/in^2	Strain in/in
2.45	4.2	62500	0.0062
2.50	4.3	63775	0.0063
2.56	4.4	65306	0.0065
2.61	4.5	66581	0.0066
2.675	4.6	68239	0.0068
2.73	4.7	69642	0.0069
2.79	2.8	71173	0.0071
2.83	4.9	72193	0.0072
2.90	5.0	73979	0.0074
2.95	5.1	75255	0.0075
3.00	5.2	76530	0.0077
3.01	5.3	76785	0.0078
3.03	5.4	77295	0.0080
3.05	5.5	77806	0.0081
3.061	5.6	78086	0.0083
3.061	5.7	78086	0.0084
3.061	5.8	78086	0.0086
3.061	5.9	78086	0.0087
3.061	6.0	78086	0.0088
3.061	6.1	78086	0.0090

TABLE 5

The initial single amplitude cyclic history of cycle number, load, stress, and relaxation rate coefficient in a uniaxial specimen.

Cycle No.	Load volts	Stress, lbf/in^2	Relaxation Rate Coef.
1	2.887	73647	0.09777
2	2.855	72831	0.60619
3	2.853	72780	0.42748
4	2.849	72678	0.35569
5	2.846	72602	0.30562
6	2.845	72567	0.26054
7	2.845	72567	0.22332
8	2.844	72551	0.19980
9	2.846	72602	0.16979
10	2.845	72577	0.15633
11	2.843	72525	0.14851
12	2.844	72551	0.13320
13	2.843	72525	0.12566
14	2.845	72576	0.11169
15	2.846	72602	0.10187
16	2.844	72551	0.09990
17	2.841	72474	0.10023
18	2.842	72500	0.09271
19	2.842	72500	0.08783
20	2.840	72449	0.08696
21	2.839	72432	0.08449
22	2.840	72448	0.07905
23	2.840	72448	0.07561
24	2.840	72448	0.07246
25	2.840	72448	0.06957
26	2.839	72423	0.06825
27	2.838	72397	0.06702
28	2.837	72372	0.06589
29	2.839	72423	0.06119
30	2.839	72423	0.05915
31	2.837	72372	0.05951
32	2.838	72397	0.05655
33	2.839	72423	0.05377
34	2.838	72397	0.05322
35	2.841	72474	0.04868
36	2.841	72474	0.04733
37	2.842	72500	0.04510
38	2.842	72500	0.04391
39	2.840	72448	0.04459
40	2.842	72500	0.04171
41	2.842	72500	0.04070
42	2.842	72500	0.03973
43	2.841	72474	0.03963
44	2.842	72500	0.03793
45	2.840	72448	0.03865

Cycle No.	Load volts	Stress lbf/in^2	Relaxation Rate Coef.
46	2.841	72474	0.03704
47	2.838	72397	0.03850
48	2.841	72474	0.03550
49	2.837	72372	0.03765
50	2.838	72397	0.03619
51	2.837	72372	0.03617
52	2.838	72397	0.03840
53	2.838	72397	0.03414
54	2.838	72397	0.03351
55	2.834	72295	0.03547
56	2.832	72244	0.03609
57	2.830	72193	0.03670
58	2.825	72066	0.03912
59	2.824	72040	0.03905
60	2.822	71989	0.03958
61	2.821	71964	0.03952
62	2.820	71938	0.03945
63	2.822	71989	0.03770
64	2.823	72015	0.03656
65	2.820	71938	0.03763
66	2.821	71964	0.03652
67	2.821	71964	0.03598
68	2.820	71938	0.03597
69	2.819	71913	0.03596
70	2.819	71913	0.03545
71	2.820	71938	0.03445
72	2.821	71964	0.03348
73	2.819	71913	0.03399
74	2.820	71938	0.03305
75	2.823	72015	0.03119
76	2.823	72105	0.03078
77	2.824	72040	0.02993
78	2.825	72066	0.02909
79	2.823	72015	0.02961
80	2.822	71989	0.02969
81	2.824	72040	0.02845
82	2.823	72015	0.02853
83	2.822	71989	0.02861
84	2.823	72015	0.02785
85	2.823	72015	0.02752
86	2.823	72015	0.02720
87	2.825	72066	0.02608
88	2.819	71913	0.02820
89	2.823	72015	0.02629
90	2.819	71913	0.02757
91	2.823	72015	0.02571
92	2.822	71989	0.02581
93	2.822	71989	0.02554
94	2.820	71938	0.02602
95	2.821	71964	0.02537
96	2.823	72015	0.02437

Cycle No.	Load volts	Stress lbf/in^2	Relaxation Rate Coef.
97	2.820	71938	0.02522
98	2.820	71938	0.02496
99	2.818	71887	0.02542
100	2.818	71887	0.02517
102	2.819	71913	0.02433
104	2.817	71862	0.02454
106	2.818	71887	0.02374
108	2.819	71913	0.02298
110	2.819	71913	0.02256
112	2.818	71887	0.02247
114	2.817	71862	0.02239
116	2.818	71887	0.02170
118	2.821	71964	0.02043
120	2.819	71913	0.02068
122	2.818	71887	0.02063
124	2.819	71913	0.02001
126	2.821	71964	0.01913
128	2.819	71913	0.01939
130	2.821	71964	0.01854
132	2.822	71989	0.01799
134	2.820	71938	0.01825
136	2.819	71913	0.01825
138	2.820	71938	0.01772
140	2.819	71913	0.01772
142	2.822	71989	0.01673
144	2.822	71989	0.01649
146	2.822	71989	0.01627
148	2.822	71989	0.01605
150	2.822	71989	0.01583

TABLE 6

The second single amplitude cyclic history of cycle number, load, stress, and relaxation rate coefficient on a uniaxial speimen.

Cycle No.	Load volts	Stress $_2$ lbf/in^2	Relaxation Rate Coef.
1	2.957	75433	0.10113
2	2.920	74489	0.68015
3	2.912	74285	0.54488
4	2.905	74107	0.46883
5	2.902	74030	0.39573
6	2.900	73979	0.34126
7	2.901	74005	0.28759
8	2.894	73826	0.28184
9	2.894	73826	0.25052
10	2.889	73698	0.24276
11	2.893	73801	0.20811
12	2.888	73673	0.20519
13	2.882	73520	0.20540
14	2.886	73622	0.18082
15	2.884	73571	0.17339
16	2.886	73622	0.15822
17	2.885	73596	0.15095
18	2.886	73622	0.14064
19	2.885	73596	0.13506
20	2.887	73647	0.12484
21	2.885	73596	0.12220
22	2.884	73571	0.11822
23	2.885	73596	0.11157
24	2.885	73596	0.10692
25	2.884	73571	0.10403
26	2.885	73596	0.09870
27	2.882	73520	0.09890
28	2.884	73571	0.09289
29	2.883	73545	0.09088
30	2.886	73622	0.08438
31	2.882	73520	0.08614
32	2.885	73596	0.08019
33	2.881	73494	0.08197
34	2.884	73571	0.07650
35	2.879	73443	0.07927
36	2.882	73520	0.07417
37	2.880	73469	0.07404
38	2.880	73469	0.07210
39	2.885	73596	0.06580
40	2.879	73443	0.06936
41	2.877	73392	0.06936
42	2.876	73367	0.06854
43	2.879	73443	0.06452
44	2.881	73494	0.06148
45	2.880	73469	0.06088

Cycle No.	Load volts	Stress lbf/in^2	Relaxation Rate Coef.
46	2.880	73469	0.05956
47	2.881	73494	0.05755
48	2.881	73494	0.05635
49	2.879	73443	0.05662
50	2.879	73443	0.05549
51	2.880	73469	0.05372
52	2.881	73494	0.05202
53	2.882	73520	0.05038
54	2.881	73494	0.05009
55	2.880	73469	0.04981
56	2.878	73418	0.05016
57	2.882	73520	0.04685
58	2.882	73520	0.04604
59	2.883	73545	0.04467
60	2.882	73520	0.04450
61	2.880	73469	0.04491
62	2.882	73520	0.04307
63	2.880	73469	0.04349
64	2.878	73418	0.04389
65	2.879	73443	0.04268
66	2.881	73494	0.04098
67	2.880	73469	0.04089
68	2.879	73443	0.04079
69	2.883	73545	0.03820
70	2.877	73392	0.04063
71	2.879	73443	0.03908
72	2.881	73494	0.03757
73	2.878	73418	0.03848
74	2.879	73443	0.03749
75	2.878	73418	0.03746
76	2.881	73494	0.03559
77	2.881	73494	0.03513
78	2.883	73545	0.03379
79	2.882	73520	0.03380
80	2.882	73520	0.03338
81	2.882	73520	0.03297
82	2.878	73418	0.03426
83	2.880	73469	0.03301
84	2.880	73469	0.03261
85	2.878	73418	0.03305
86	2.880	73469	0.03186
87	2.879	73443	0.03189
88	2.876	73367	0.03271
89	2.880	73469	0.03078
90	2.880	73469	0.03044
91	2.880	73469	0.03011
92	2.878	73418	0.03053
93	2.879	73443	0.02983
94	2.881	73494	0.02878
95	2.880	73469	0.02884
96	2.878	73418	0.02926

Cycle No.	Load volts	Stress, lbf/in^2	Relaxation Rate Coef.
97	2.878	73418	0.02896
98	2.881	73494	0.02760
99	2.880	73469	0.02767
100	2.880	73469	0.02740
102	2.880	73469	0.02686
104	2.880	73469	0.02634
106	2.877	73392	0.02683
108	2.878	73418	0.02601
110	2.878	73418	0.02554
112	2.878	73418	0.02508
114	2.879	73443	0.02434
116	2.877	73392	0.02452
118	2.878	73418	0.02381
120	2.877	73392	0.02370
122	2.877	73392	0.02331
124	2.876	73367	0.02322
126	2.878	73418	0.02229
128	2.877	73392	0.02222
130	2.876	73367	0.02214
132	2.879	73443	0.02102
134	2.880	73469	0.02044
136	2.879	73443	0.02040

TABLE 7

The fourth single amplitude cyclic history of cycle number, load, stress, and relaxation rate coefficient on a uniaxial specimen.

Cycle No.	Load volts	Stress lbf/in^2	Relaxation Rate Coef.
1	3.024	77142	0.07404
2	2.980	76020	0.76988
3	2.971	75790	0.61408
4	2.967	75790	0.46056
5	2.968	75714	0.39539
6	2.968	75714	0.32388
7	2.967	75688	0.28242
8	2.969	75739	0.23870
9	2.971	75790	0.20469
10	2.970	75765	0.18759
11	2.967	75688	0.17972
12	2.965	75637	0.17037
13	2.965	75637	0.15726
14	2.968	75714	0.13880
15	2.968	75714	0.12955
16	2.967	75688	0.12356
17	2.965	75637	0.12026
18	2.967	75688	0.10983
19	2.969	75739	0.10050
20	2.967	75688	0.09885
21	2.969	75739	0.09093
22	2.968	75714	0.08833
23	2.967	75688	0.08595
24	2.967	75688	0.08237
25	2.966	75663	0.08043
26	2.966	75663	0.07733
27	2.966	75663	0.07447
28	2.966	75663	0.07181
29	2.966	75663	0.06933
30	2.969	75739	0.06365
31	2.966	75663	0.06486
32	2.964	75612	0.06494
33	2.966	75663	0.06093
34	2.966	75663	0.05914
35	2.964	75612	0.05937
36	2.963	75586	0.05866
37	2.967	75688	0.05343
38	2.965	75637	0.05380
39	2.964	75612	0.05329
40	2.966	75663	0.05027
41	2.965	75637	0.04986
42	2.963	75586	0.05028
43	2.965	75637	0.04754
44	2.963	75586	0.04799
45	2.964	75612	0.04618

Cycle No.	Load volts	Stress lbf/in^2	Relaxation Rate Coef.
46	2.967	75688	0.04298
47	2.966	75663	0.04278
48	2.968	75714	0.04048
49	2.970	75765	0.03828
50	2.967	75688	0.03954
51	2.966	75663	0.03942
52	2.969	75739	0.03672
53	2.969	75739	0.03603
54	2.970	75765	0.03474
55	2.968	75714	0.03533
56	2.966	75663	0.03590
57	2.969	75739	0.03350
58	2.968	75714	0.03350
59	2.967	75688	0.03351
60	2.968	75714	0.03239
61	2.966	75663	0.03296
62	2.967	75688	0.03189
63	2.967	75688	0.03138
64	2.966	75663	0.03142
65	2.967	75688	0.03041
66	2.966	75663	0.03046
67	2.967	75688	0.02951
68	2.967	75688	0.02907
69	2.965	75637	0.02963
70	2.965	75637	0.02921
71	2.962	75561	0.03022
72	2.961	75535	0.03027
73	2.965	75637	0.02801
74	2.962	75561	0.02899
75	2.962	75561	0.02861
76	2.962	75561	0.02823
77	2.963	75586	0.02743
78	2.963	75586	0.02708
79	2.962	75561	0.02716
80	2.963	75586	0.02640
81	2.963	75586	0.02607
82	2.965	75637	0.02493
83	2.961	75535	0.02627
84	2.961	75535	0.02595
85	2.961	75535	0.02564
86	2.961	75535	0.02534
87	2.962	75561	0.02466
88	2.962	75561	0.02438
89	2.963	75586	0.02373
90	2.963	75586	0.02347
91	2.961	75535	0.02395
92	2.963	75586	0.02296
93	2.960	75510	0.02380
94	2.962	75561	0.02283
95	2.961	75535	0.02294
96	2.963	75586	0.02200

Cycle No.	Load volts	Stress lbf/in^2	Relaxation Rate Coef.
97	2.961	75535	0.02247
98	2.962	75561	0.02189
99	2.961	75535	0.02201
100	2.962	75561	0.02146
102	2.961	75535	0.02137
104	2.958	75459	0.02193
106	2.960	75510	0.02088
108	2.959	75484	0.02081
110	2.960	75510	0.02012
112	2.960	75510	0.01976
114	2.959	75484	0.01971
116	2.960	75510	0.01925
118	2.959	75484	0.01904
120	2.958	75459	0.01901
122	2.958	75459	0.01842
124	2.958	75459	0.01839
126	2.958	75459	0.01810
128	2.957	75433	0.01808
130	2.959	75484	0.01728
132	2.957	75433	0.01753
134	2.958	75459	0.01702
136	2.956	75408	0.01727
138	2.956	75408	0.01702
140	2.958	75459	0.01629
142	2.957	75433	0.01630
144	2.957	75433	0.01607
146	2.955	75382	0.01632
148	2.955	75382	0.01610
150	2.958	75459	0.01521

TABLE 8

Anelastic strain-time data on a uniaxial specimen with initial strain hold at 0.00504 in/in

Time min.	Strain in/in X 10^2
0.0	0.5400
3.0	0.5370
4.0	0.5344
5.0	0.5328
6.0	0.5319
8.0	0.5256
10.0	0.5219
12.0	0.5194
15.0	0.5127
25.0	0.5083
35.0	0.5076
40.0	0.5051
45.0	0.5034
50.0	0.5034
55.0	0.5033
80.0	0.5021
85.0	0.5021

TABLE 9.

Anelastic strain-time data on a uniaxial specimen with initial strain hold at 0.00504 in/in

Time min.	Strain in/in X 10^2
0.0	0.5046
1.0	0.5009
2.0	0.4978
3.0	0.4938
4.0	0.4900
5.0	0.4888
8.0	0.4871
10.0	0.4864
12.0	0.4861
14.0	0.4857
16.0	0.4849
20.0	0.4844
25.0	0.4836
30.0	0.4824
35.0	0.4809
40.0	0.4799
45.0	0.4791
50.0	0.4784
60.0	0.4786
70.0	0.4786
80.0	0.4785
90.0	0.4785

TABLE 10

Cycle No.,load, stress, and relaxation rate coefficient data from single amplitude cyclic loading test on a uniaxial specimen.(Strain range 0.0012 in/in to 0.0025 in/in)

Cycle No.	Load volts	Stress lbf/in^2	Relaxation Rate Coef.
1	0.579	14770	0.20014
3	0.577	14719	0.18206
5	0.579	14770	0.04003
7	0.578	14744	0.05328
9	0.579	14770	0.02224
11	0.580	14795	0.00251
13	0.578	14744	0.02869
15	0.580	14795	0.00184
17	0.580	14795	0.00162
19	0.576	14693	0.03788
21	0.578	14744	0.01776
23	0.580	14795	0.00120
25	0.578	14744	0.01492
27	0.579	14770	0.00741
29	0.576	14693	0.02481
31	0.578	14744	0.01203
33	0.577	14719	0.01655
35	0.578	14744	0.01066
37	0.575	14668	0.02415
39	0.577	14719	0.01400
41	0.579	14770	0.00488
43	0.580	14795	0.00064
45	0.580	14795	0.00061
47	0.578	14744	0.00794
49	0.577	14719	0.01115
51	0.577	14719	0.01071
53	0.579	14770	0.00378
55	0.579	14770	0.00364
57	0.579	14770	0.00351
59	0.578	14744	0.00632
61	0.580	14795	0.00045
63	0.579	14770	0.00318
65	0.580	14795	0.00042
67	0.579	14770	0.00299
69	0.577	14719	0.00792
71	0.577	14719	0.00769
73	0.579	14770	0.00274
75	0.580	14795	0.00037
77	0.579	14770	0.00260
79	0.579	14770	0.00253
81	0.574	14642	0.01319
83	0.578	14744	0.00449
85	0.580	14795	0.00032
87	0.578	14744	0.00429

Cycle No.	Load volts	Stress lbf/in^2	Relaxation Rate Coef.
89	0.579	14770	0.00225
91	0.577	14719	0.00600
93	0.578	14744	0.00401
95	0.577	14719	0.00575
97	0.575	14668	0.00921
99	0.577	14719	0.00552
101	0.578	14744	0.00369
103	0.577	14719	0.00530
105	0.578	14744	0.00355
107	0.578	14744	0.00349
109	0.578	14744	0.00342
111	0.576	14693	0.00648
113	0.579	14770	0.00177
115	0.578	14744	0.00324
117	0.577	14719	0.00467
119	0.576	14693	0.00605
121	0.577	14719	0.00451
123	0.576	14693	0.00585
125	0.576	14693	0.00576

TABLE 11

Cycle No., load, stress, and relaxation rate coefficient data from single amplitude cyclic loading test on a uniaxial specimen.(Strain range 0.0024 in/in to 0.005 in/in)

Cycle No.	Load volts	Stress lbf/in^2	Relaxation Rate Coef.
1	1.577	40229	0.19967
3	1.573	40127	0.15121
5	1.569	40025	0.14165
7	1.562	39846	0.16506
9	1.563	39872	0.12127
11	1.560	39795	0.11668
13	1.562	39846	0.08887
15	1.560	39795	0.08557
17	1.556	39693	0.09060
19	1.558	39744	0.07431
21	1.561	39821	0.05807
23	1.560	39795	0.05581
25	1.551	39566	0.07448
27	1.561	39821	0.04516
29	1.560	39795	0.04426
31	1.552	39591	0.05799
33	1.555	39668	0.04862
35	1.557	39719	0.04217
37	1.551	39566	0.05033
39	1.556	39693	0.03949
41	1.556	39693	0.03757
43	1.547	39464	0.04931
45	1.553	39617	0.03852
47	1.554	39642	0.03551
49	1.546	39438	0.04459
51	1.554	39624	0.03272
53	1.552	39591	0.03392
55	1.550	39540	0.03503
57	1.553	39617	0.03041
59	1.552	39591	0.03047
61	1.551	39566	0.03053
63	1.548	39489	0.03263
65	1.548	39489	0.03163
67	1.550	39540	0.02876
69	1.545	39413	0.03260
71	1.550	39540	0.02714
73	1.543	39362	0.03259
75	1.551	39566	0.02483
77	1.548	39489	0.02670
79	1.551	39566	0.02357
81	1.551	39566	0.02300

TABLE 12

Cycle No., load, stress, and relaxation rate coefficient data from single amplitude cyclic loading test on a uniaxial specimen.(Strain range 0.0049 in/in to 0.0076 in/in)

Cycle No.	Load volts	Stress lbf/in^2	Relaxation Rate Coef.
1	2.515	64158	0.22083
3	2.504	63877	0.21972
5	2.503	63852	0.13982
7	2.503	63852	0.09987
9	2.501	63801	0.08656
11	2.500	63775	0.07446
13	2.500	63775	0.06300
15	2.502	63826	0.04927
17	2.502	63826	0.04347
19	2.502	63826	0.03890
21	2.502	63826	0.03519
23	2.501	63801	0.03387
25	2.501	63801	0.03116
27	2.501	63801	0.02885
29	2.501	63801	0.02686
31	2.500	63775	0.02642
33	2.501	63801	0.02361
35	2.501	63801	0.02226
37	2.497	63698	0.02538
39	2.496	63673	0.02511
41	2.493	63596	0.02682
43	2.494	63622	0.02464
45	2.493	63596	0.02443
47	2.493	63596	0.02339
49	2.490	63520	0.02489
51	2.491	63545	0.02313
53	2.491	63545	0.02226
55	2.493	63596	0.01999
57	2.493	63596	0.01929
59	2.493	63596	0.01863
61	2.492	63571	0.01868
63	2.490	63520	0.01936
65	2.490	63520	0.01877
67	2.492	63571	0.01701
69	2.490	63520	0.01768
71	2.490	63520	0.01718
73	2.491	63545	0.01616
75	2.489	63494	0.01680
77	2.490	63520	0.01584
79	2.487	63443	0.01697
81	2.489	63494	0.01556
83	2.486	63418	0.01663
85	2.486	63418	0.01624
87	2.487	63443	0.01541

Cycle No.	Load volts	Stress lbf/in^2	Relaxation Rate Coef.
89	2.489	63494	0.01416
91	2.489	63494	0.01385
93	2.490	63520	0.01312
95	2.493	63596	0.01157
97	2.493	63596	0.01133
99	2.497	63698	0.00949
101	2.497	63698	0.00930
103	2.498	63724	0.00873
105	2.497	63698	0.00894
107	2.498	63724	0.00840
109	2.497	63698	0.00862
111	2.499	63750	0.00774
113	2.497	63698	0.00831
115	2.496	63673	0.00851
117	2.495	63647	0.00871
119	2.495	63647	0.00857
121	2.494	63622	0.00875
123	2.492	63571	0.00926
125	2.490	63520	0.00976
127	2.485	63392	0.01119
129	2.490	63520	0.00946
131	2.494	63622	0.00809
133	2.487	63443	0.01008
135	2.486	63418	0.01023
137	2.487	63443	0.00978
139	2.492	63571	0.00820
141	2.492	63571	0.00808
143	2.492	63571	0.00797
145	2.482	63316	0.01061
147	2.487	63443	0.00912
149	2.492	63571	0.00765

TABLE 13

Monotonic stress and strain data from a dual amplitude cyclic loading test on a uniaxial specimen.

Load volts	Strain volts	Stress $_2$ lbf/in^2	Strain in/in
0.00	0.0	0	0.0000
0.11	0.2	2806	0.0003
0.24	0.4	6122	0.0006
0.36	0.6	9183	0.0009
0.48	0.8	12245	0.0012
0.60	1.0	15306	0.0015
0.90	1.5	22959	0.0022
1.21	2.0	30867	0.0029
1.51	2.5	38520	0.0037
1.81	3.0	46173	0.0044
2.10	3.5	53571	0.0052
2.39	4.0	60969	0.0059
2.50	4.2	63775	0.0062
2.61	4.4	66582	0.0065
2.66	4.5	67857	0.0066
2.70	4.6	68877	0.0068
2.73	4.7	69942	0.0069
2.78	4.8	70718	0.0071
2.80	4.9	71428	0.0072
2.82	5.0	71939	0.0074
2.85	5.2	72704	0.0077
2.89	5.5	73724	0.0081
2.90	5.6	73980	0.0083

TABLE 14

Cycle No., load, stress, and relaxation rate coefficient data from a dual amplitude cyclic loading test on a uniaxial specimen.

Cycle No.	Load volts		Stress lbf/in^2		Relaxation Rate Coef.	
	Hi	Low	Hi	Low	Hi	Low
1	2.728		69591		0.01173	
2		1.370		34948		0.07294
3	2.712		69183		0.19999	
4		1.364		34795		0.14620
5	2.715		69260		0.09718	
6		1.350		34438		0.26941
7	2.713		69209		0.08044	
8		1.352		34489		0.18356
9	2.71		69132		0.07486	
10		1.351		34464		0.15424
11	2.713		69209		0.05119	
12		1.349		34413		0.14088
13	2.712		69183		0.04615	
14		1.350		34438		0.11546
15	2.714		69234		0.03508	
16		1.348		34387		0.11030
17	2.713		69209		0.03312	
18		1.350		34438		0.08981
19	2.715		69260		0.02576	
20		1.358		34642		0.05128
21	2.713		69209		0.02681	
22		1.350		34438		0.07348
23	2.710		69132		0.02929	
24		1.350		34438		0.06735
25	2.709		69107		0.02843	
26		1.349		34413		0.06502
27	2.711		69158		0.02359	
28		1.347		34362		0.06568
29	2.711		69158		0.02196	
30		1.350		34438		0.05388
31	2.712		69183		0.01935	
32		1.347		34362		0.05747
33	2.710		69132		0.02042	
34		1.358		34642		0.03017
35	2.708		69081		0.02136	
36		1.348		34387		0.04902
37	2.711		69158		0.01721	
38		1.349		34413		0.04449
39	2.712		69183		0.01538	
40		1.350		34438		0.04041
41	2.71		69132		0.01643	
42		1.351		34464		0.03672
43	2.708		69081		0.01739	
44		1.353		34515		0.03169
45	2.705		69005		0.01908	

Cycle No.	Load volts		Stress lbf/in^2		Relaxation Rate Coef.	
	Hi	Low	Hi	Low	Hi	Low
46		1.350		34438		0.03514
47	2.706		69030		0.01748	
48		1.348		34387		0.03677
49	2.705		69005		0.01752	
50		1.349		34413		0.03381
51	2.704		68979		0.01756	
52		1.347		34362		0.03536
53	2.705		69005		0.01620	
54		1.350		34438		0.02994
55	2.704		68979		0.01628	
56		1.347		34362		0.03284
57	2.705		69005		0.01506	
58		1.340		34183		0.04070
59	2.701		68903		0.01706	
60		1.336		34081		0.04432
61	2.698		68826		0.01832	
62		1.325		33801		0.05622
63	2.697		68801		0.01833	
64		1.327		33852		0.05211
65	2.691		68647		0.02119	
66		1.325		33801		0.05281
67	2.700		68877		0.01557	
68		1.323		33750		0.05348
69	2.695		68750		0.01781	
70		1.322		33724		0.05303
71	2.696		68775		0.01678	
72		1.322		33724		0.05156
73	2.691		68647		0.01887	
74		1.322		33724		0.05017
75	2.690		68622		0.01886	
78		1.315		33545		0.05440
81	2.688		68571		0.01838	
84		1.300		33163		0.06417
87	2.681		68392		0.02011	
90		1.306		33316		0.05478
93	2.674		68214		0.02162	
96		1.308		33367		0.04976
99	2.670		68112		0.02183	
102		1.312		33469		0.04384
105	2.667		68035		0.02165	
108		1.311		33443		0.04211
111	2.666		68010		0.02082	
114		1.311		33443		0.03989
117	2.664		67959		0.02039	
120		1.305		33290		0.04172
123	2.665		67984		0.01909	
126		1.306		33316		0.03913
129	2.662		67908		0.01908	
132		1.305		33290		0.03793
135	2.666		68010		0.01712	
138		1.306		33316		0.03572

Cycle No.	Load volts		Stress lbf/in^2		Relaxation Rate Coef.	
	Hi	Low	Hi	Low	Hi	Low
141	2.660		67857		0.01799	
144		1.307		33341		0.03370
147	2.660		67857		0.01725	
150		1.304		33265		0.03389

LIST OF REFERENCES

1. Simkins, D., Neulieb, R. L. and Golden, D. J., "Load-Time Dependent Relaxation of Residual Stresses," Journal of Aircraft, v. 9, No. 12, p. 867-868, 12 December 1972.

2. Potter, J. M., "The Effect of Load Interaction and Sequence on the Fatigue Behavior of Notched Coupons," Cyclic Stress-Strain Behavior-Analysis, Experimentation, and Failure Prediction, ASTM STP 519, p. 124-132, 1973.

3. University of Illinois, Department of Theoretical and Applied Mechanics T. & A.M. Report No. 383, A History Dependent Parameter for the Cyclic Stress-Strain Behavior of Metals, by Jhansale, March 1974.

4. The Boeing Company Commercial Airplane Division Document No. D6-23733, Strain-Cycling Effects in 1100 Aluminum, by Harry A. Moreen, November 1968.

5. Dieter, G.E., Mechanical Metallurgy, 2d ed., p. 487-489, McGraw-Hill Book Company, 1976.

6. ASTM, Annual Book of ASTM Standards Part 10, "Tentative Recommended Practice for Constant Amplitude Axial Fatigue Tests of Metallic Material," p.E466-72T, 1975.

7. MTS Systems Corporation, Operator's Manual, Series 810, Material Test System, No. 976.01-30.

8. Volterra, E. and Zachmanoglov, E. C., Dynamics of Vibrations, p. 15-17, Charles E. Merril Books, Inc., 1965.

9. Horne, G. M., An Investigation of Stress Determination for Aircraft Fatigue Life Estimation from In-Flight Strain Data, Master's Thesis, Naval Postgraduate School, Monterey, California, September 1976.

INITIAL DISTRIBUTION LIST

		No. Copies
1.	Defense Documentation Center Cameron Station Alexandria, Virginia 22314	2
2.	Library, Code 0142 Naval Postgraduate School Monterey, California 93940	2
3.	Department Chairman, Code 67 Department of Aeronautics Naval Postgraduate School Monterey, California 93940	1
4.	Associate Professor G. H. Lindsey, Code 67Li Department of Aeronautics Naval Postgraduate School Monterey, California 93940	1
5.	LT Richard Allen Bentley, USN 731 West 13th Street Alliance, Nebraska 69301	1

Thesis 169548
B393 Bentley
c.1 An investigation of the recovery processes in 7075-T651 aluminum responsible for a stress decay during dynamic loading histories.